

University College London
Department of Computer Science

OPTIMAL ORDER EXECUTION IN CRYPTOCURRENCY MARKETS USING DISCRETE PROPAGATOR MODELS AND LIQUIDITY FLUCTUATIONS

FQZQ7

Academic Supervisor: Professor Chris Clack
Industrial Supervisor: Dr Benjamin Loveless (JIT Strategies)

London, 07 October 2024

This dissertation is submitted as a partial requirement for the MSc Computational Finance degree at UCL. It is substantially the result of my own work except where explicitly indicated in the text. The dissertation may be freely copied and distributed, provided the source is explicitly acknowledged.

Abstract

This thesis addresses two core objectives in cryptocurrency trading: calibrating the Discrete Propagator Model (DPM) to capture market impact and optimising trade execution schedules using high-frequency data from the Kraken exchange. The study leverages a sliding-window cross-validation approach to account for short-term market dynamics and intraday liquidity fluctuations in Bitcoin trading. Despite successfully capturing some features of liquidity variations, the DPM falls short in explaining price movements based solely on traded volume, as indicated by consistently low R^2 values in test windows. This highlights a key limitation of the model in the cryptocurrency context, where market behaviours differ from traditional assets. The second objective focuses on optimising trading schedules by minimising execution costs using the calibrated parameters. While the model has predictive limitations, the optimised schedules result in significant cost savings, averaging 35.55% when compared to industry benchmarks like TWAP, VWAP, and Market Open strategies. These findings suggest that, even with reduced predictive accuracy, the DPM framework can still offer valuable insights for cost-efficient execution in volatile cryptocurrency markets.

Contents

List of Acronyms	iii
List of Figures	v
List of Symbols	vi
List of Tables	vii
1 Introduction	1
2 Literature Review	3
2.1 Price Impact	3
2.2 Price Manipulation	4
2.3 Optimal Execution Strategy	6
2.4 Temporary and Permanent Price Impact	8
2.5 Transient Price Impact	9
2.5.1 General Transient Impact Model	10
2.5.2 Linear Transient Impact: Obizhaeva-Wang Model	10
2.6 Limitations of the Transient Impact Model	11
2.7 Moving Towards the Discrete Propagator Model	12
2.8 The Bitcoin Market	15
3 Data Preparation	17
3.1 Motivation	17
3.2 Tardis Data	17
3.3 Data Normalisation	20
4 Model Calibration	23
4.1 Methodology	23
4.2 Calibration Results	24
4.2.1 Observations	24
4.2.2 Variations in λ Throughout our Dataset	26
4.2.3 Optimising for δ	28
5 Optimal Trade Scheduling	31
5.1 Excess Cost Minimisation	31
5.2 Fixed Intraday Illiquidity	32

5.2.1	Linear Impact Case	32
5.2.2	Non-linear Impact Case	34
5.2.3	Optimal Trading Schedule Across (δ, λ) Combinations	35
5.2.4	Optimal Trading Schedule Across Trading Frequencies	37
5.2.5	Optimal Trading Schedule Across Bid-Ask Spreads	39
5.3	Time-Dependent Intraday Illiquidity	42
5.4	Summary	45
6	Conclusion	47
6.1	Conclusion	47
6.2	Future Work	47

List of Acronyms

AC Almgren and Chriss Model

ADV Average Daily Volume

BTC Bitcoin

DPM Discrete Propagator Model

HFT High-Frequency Trading

LOB Limit Order Book

OFI Order-Flow Imbalance

OW Obizhaeva-Wang Model

SLSQP Sequential Least Squares Quadratic Programming

SMA Simple Moving Average

TIM Transient Impact Model

TWAP Time Weighted Average Price

VWAP Volume Weighted Average Price

List of Figures

1	Plot of cumulative signed volume throughout the day (top) and plot of total volume $\sum_{t_{n-1} < t \leq t_n} v_t$ vs. absolute of net signed volume $ \Delta F_n $ (bottom) for the 2024-05-05 trading day. Both plots use 15-minute bins for better visualisation.	20
2	Comparison of daily volume with the 30-day SMA of volume, calculated using $V_{avg}(m, k)$ (left), and comparison of σ with the 30-Day SMA of standard deviations of binned return, calculated using $\sigma_{ret}(m, k)$ (right).	22
3	Visualisation of the intraday training and testing R^2 scores alongside the corresponding intraday λ_t values for various end-of-training dates, and using the optimal exponent $\delta = 0.35$. Training period is 7 days, testing period is 3 days. The UTC timezone is used throughout the analysis [45].	25
4	Heatmap showing the λ_t values across different end-of-training periods (left) and plot of the mean daily λ_t over the entire dataset (right). Both plots use the exponent $\delta = 0.35$ and identical training-testing periods.	27
5	Train R^2 for different values of δ over time.	28
6	The optimal execution strategy calculated using the SLSQP method for $X_0 = 0.1$. The time horizon T is divided into 96 distinct time bins, corresponding to 4 trading intervals per hour over a 24-hour period. The y-axis represents the consistent average trading rate within each sub-interval. The minimum estimated expected execution cost is 5.59×10^{-4}	34
7	The optimal execution strategy determined using the SLSQP method for $X = 0.1$. The time horizon T is discretised into 96 time bins, with 4 trading intervals per hour over a full 24-hour period. The y-axis represents the average volume traded per time bin, illustrating the optimal rate of execution under different non-linearity exponents.	35
8	Optimal trading schedule for different combinations of δ and $\bar{\lambda}$. Each subplot illustrates the optimal volume distribution over 15-minute intervals during a trading day. The top left subplot corresponds to $(\delta, \bar{\lambda}) = (0.7, 40.54)$, the top right to $(0.5, 15.05)$, the bottom left to $(0.3, 3.99)$, and the bottom right to $(0.1, 0.52)$	36
9	Optimal trading schedule for different time bin frequencies: 60, 45, 30, 20, 10, and 5 minutes. The propagator model parameters are set to $\delta = 0.5$, $\lambda \approx 15.05$, and a half-life of 1 hour.	37
10	Optimal execution costs as a function of the degree of non-linearity, δ , across different trading frequencies. The range $\delta \in \{0.4, 0.5, \dots, 1.0\}$ is used. The impact coefficient $\bar{\lambda}$ is fixed, corresponding to $\delta = 0.5$	38

11	Optimal trading schedules under different bid-ask spread costs (0, 10, 25, 50, and 100 basis points) for $(\delta, \bar{\lambda}) = (0.5, 15.05)$. The subplots illustrate how increasing spread costs affect the distribution of trading volumes across time bins. The expected execution cost is shown for each case, and the final subplot displays only non-negative volumes traded within each time bin.	40
12	Daily mean bid-ask spread for the BTC/USD exchange rate over our dataset. The daily mean bid-ask spread is measured in basis points (bps), calculated as the difference between the best ask and bid quote prices normalised by the mid-price.	41
13	The optimal trading schedule for BTC/USD using historical volume data from July 1, 2024, comparing $\bar{\lambda} = 5.83$ (top left) and λ_t (bottom left). The bar plots show the volume traded in each time bin, while the red line depicts λ values. The strategy assumes $\delta = 0.35$ and $X = 0.1$, with a 15-minute time bin frequency. VWAP strategy for BTC/USD using historical volume data from July 25, 2024 (right). The volume traded in each bin is based on the VWAP calculation, with a 15-minute time bin frequency.	42

List of Symbols

X	Total volume to be executed
S_t	Asset price at time t
δ	Non-linearity exponent of the price impact function
λ	Illiquidity parameter
$\bar{\lambda}$	Mean illiquidity over time
λ_t	Time-dependent illiquidity parameter
Δt	Time step duration
σ	Standard deviation of returns
β	Decay parameter for impact dissipation
V_{avg}	Average traded volume over a defined period
R^2	Coefficient of determination for model fit

List of Tables

1	Kraken trades-and-quotes file formats.	18
2	Hourly λ_t values with corresponding train R^2 and test R^2 using 7 days of training followed by 3 sequential days of testing for $\delta = 0.1$. The train period ends on June 04, 2024.	25
3	These values reflect the total negative volume observed in the optimal trading schedules.	40
4	Execution cost comparison across various trading strategies for total volumes $X \in \{0.025, 0.05, 0.1, 0.25\}$. All results are calculated with fixed value $\delta = 0.35$. Only the "Constant" strategy uses the fixed value $\bar{\lambda} = 6.50$	44
5	Relative savings of using the Intraday λ_t strategy compared to industry benchmarks TWAP, VWAP, Market Open and Constant $\bar{\lambda}$ across different volumes X	45

1 Introduction

Centralised exchanges have historically been fundamental to the trading of financial products, serving as a platform where buyers and sellers could meet to execute trades. Traditionally, this process involved traders and brokers physically present on trading floors, verbally negotiating on behalf of clients who placed orders over the phone. With the rise of technology, this manual method has largely been replaced by electronic markets, offering faster, more precise, and transparent order execution. One key example of such a system is the limit order book (LOB), where market makers publicly post offers for the volumes and prices at which they are willing to trade. Traders seeking immediate execution match these offers, thereby taking liquidity from the LOB and influencing the best bid or offer price. As a result, executing large volumes in such a system requires a strategic approach, necessitating a deep understanding of the relationship between traded volume and market impact.

Advances in market microstructure have led to the development of more sophisticated models of price impact. Initially, simple permanent impact models were used, but over time, more complex dynamics such as temporary and transient impacts have been introduced. The increasing availability of market data, alongside improved analytical tools, has revealed key patterns in market impact, including intraday liquidity variations, the propagation of impact over time, and concave instantaneous impact functions [11]. In particular, order-flow imbalance (OFI) has been found to accurately explain and predict price movements [39]. These models are crucial for market makers and high-frequency trading (HFT) firms, enabling them to develop sophisticated algorithms for dynamic trade execution. However, they typically require access to detailed order book data for calibration, which can pose challenges for institutions that lack such data, technical expertise, or connectivity with exchanges.

Despite these limitations, regression-based calibration techniques applied to the discrete propagator model (DPM) have shown promise, capturing many of the key features of market impact using only trade data [39]. This research seeks to build upon these findings, focusing specifically on the cryptocurrency markets, where the impact of market orders is more pronounced due to higher volatility and liquidity fluctuations. Cryptocurrencies, with their decentralised nature and susceptibility to macroeconomic influences, require tailored models to accurately capture price dynamics and the effects of market impact. By integrating advanced electronic market models and adapting them to the particular features of cryptocurrencies, this study aims to provide deeper insights into price formation mechanisms and to develop strategies for optimal trade execution in these fast-evolving markets.

This dissertation’s primary objective is twofold: first, to calibrate the DPM on

high-frequency data from the Kraken exchange, leveraging a sliding-window cross-validation approach to adapt to short-term market dynamics. We measure intraday liquidity variations and capture non-linear transient price impacts. Key findings indicate that while the DPM captures some features of intraday liquidity changes in Bitcoin trading, it fails to explain price movements solely based on traded volume, as reflected in consistently low R^2 values across test windows. This result contrasts with the application of similar models in traditional assets, raising questions about the model's generalisability to cryptocurrency markets. The second main objective is to optimise trading schedules using the calibrated parameters. Despite the model's predictive limitations, we successfully determine optimal trading strategies that achieve significant cost savings—35.55% on average—compared to standard industry benchmarks like TWAP, VWAP, and Market Open strategies.

This thesis is structured as follows: Section 1 provides an introduction to the volume scheduling problem and the challenges posed by the market impact of metaorders. Section 2 reviews key literature on both linear and non-linear impact models, establishing the foundation for the DPM. Section 3 covers data preparation, including the selection and normalization of tick-level data from the Kraken exchange. Section 4 details the model calibration process, focusing on the optimization of key parameters that influence market impact. Section 5 addresses the execution problem, presenting the development of an optimal trading schedule using the SLSQP solver. Finally, the conclusion reflects on the model's limitations, its practical applications within the industry, and potential avenues for future research.

2 Literature Review

2.1 Price Impact

In electronic markets, market participants are typically divided into two categories: liquidity takers and liquidity providers. Liquidity takers aim to execute trades at the best possible prices by matching with counterparties, whereas liquidity providers, often market makers, continuously offer quotes for both buying and selling, ensuring a steady flow of liquidity. However, large market orders can disrupt this equilibrium. When liquidity takers submit orders that exceed the available liquidity at the best bid or ask prices, they encounter *price impact*, which refers to the shift in prices due to their trading activity.

Price impact can be considered the immediate and measurable consequence of executing large orders in the market. This effect is particularly significant for large orders that cannot be filled instantaneously without moving the price unfavourably. Such orders are typically broken down into metaorders – a series of smaller trades executed over a time interval $[0, T]$, where $T > 0$ represents the total execution horizon. The total quantity traded, X_0 , is gradually unwound (for sell strategies) or built up (for buy strategies), ensuring that liquidity is absorbed over time without significantly disrupting the market. For an execution strategy $X = (X_t)_{t \in [0, T]}$, X_t represents the asset position at time $t \in [0, T]$. This strategy is nonincreasing for sell strategies ($X_{t+1} \leq X_t$) and nondecreasing for buy strategies ($X_{t+1} \geq X_t$). This ensures that the entire position is unwound in the case of a sell strategy or fully built up in the case of a buy strategy by the end of the period, i.e., $X_T = 0$ for sell strategies or $X_T = X_0$ for buy strategies.

In a LOB framework, the *bid-ask spread* (the difference between the best bid and ask prices) and the *mid-price* (the average of the best bid and ask) serve as indicators of market conditions. When a market order is larger than the available volume at the best bid or ask price, it consumes liquidity at successive price levels, causing *market impact*. For example, if a large buy order depletes liquidity at the best ask, the remaining volume must be executed at progressively higher prices, leading to temporary price shifts. This temporary *market impact* results in higher execution costs for liquidity takers.

The distinction between *price impact* and *market impact* lies in their scope. Price impact refers specifically to the effect of a single trade or sequence of trades on the immediate asset price. It captures how the price of an asset moves in response to the execution of an order. Market impact, on the other hand, is a broader concept that encompasses the overall effect of trading activity on both the price of the traded asset

and other aspects of the market, such as liquidity and volatility. It considers not just the price shifts but also how the broader market conditions, including other market participants and the liquidity environment, adjust in response to trades.

To mathematically model *price impact*, we start by assuming a baseline unaffected price level, S_0 , which represents the initial state of the asset before any trading occurs. Once the order execution strategy is implemented, the price transitions to S_X^t , which reflects the impact of trading activity at time t . In modelling price impact, we distinguish between *temporary* and *permanent* effects. Permanent impact affects all future trades by shifting the price permanently due to the overall volume traded. Temporary impact, on the other hand, influences only the current trade and is typically reversed as liquidity replenishes in the LOB.

The revenue generated from the dynamic execution strategy is

$$\mathcal{R}_T(X) = - \int_0^T S_X(t) dX_t. \quad (2.1)$$

The associated liquidation cost is

$$C_T(X) = X_0 S_0 - \mathcal{R}_T(X). \quad (2.2)$$

This framework is essential for constructing optimal execution strategies, which seek to minimise the costs of unwinding large positions while balancing the risks associated with market impact and price fluctuations. Models such as those developed by [5, 4] and others employed mean-variance optimisation and expected utility maximisation to address these trade-offs.

Finally, capturing OFI — the difference between buy and sell volume within a given period — plays a central role in understanding aggregate price impact. Studies by [9, 25] demonstrated that excess buy pressure leads to price increases, while sell pressure results in declines. Thus, OFI serves as a powerful predictor of short-term price changes, encapsulating the relationship between trade volumes and market dynamics.

2.2 Price Manipulation

Following the treatment of regularity and irregularity in Gatheral and Schied [22, Section 2], we define price manipulation strategies and their implications in the context of market impact models.

A market impact model is said to exhibit regularity when it admits well-behaved optimal order execution strategies for reasonable risk criteria. These strategies should conform to basic conditions, like monotonicity.

Additionally, regularity conditions should be formulated in a risk-neutral manner, independent of investor-specific preferences. This can be done by defining regularity in terms of expected revenues or costs. It is also essential to distinguish the effects of price impact from profitable trading strategies that might arise from trend-following behavior, as these are separate phenomena. A standard assumption in literature is that the unaffected price process S_0 behaves like a martingale, especially when drift effects are negligible over short trading horizons. This assumption was discussed in works such as [3, 23, 36].

A key aspect of regularity is the absence of price manipulation strategies. Such strategies exploit price impact in a favourable way, generating positive expected revenues through round-trip trades.

Definition 1 (Price Manipulation Strategy). *A round trip is an order execution strategy X with $X_0 = X_T = 0$. A price manipulation strategy is a round trip X with strictly positive expected revenues,*

$$\mathbb{E}[\mathcal{R}_T(X)] > 0. \quad (2.3)$$

In models that admit price manipulation, traders could exploit the price impact to generate arbitrarily large expected profits. This becomes problematic, especially for risk-neutral investors, as it could lead to the absence of optimal execution strategies.

Price manipulation, although related to arbitrage, differs in the sense that manipulation generates average profits over time, while arbitrage guarantees profits in an almost-sure sense. Huberman and Stanzl [29] demonstrated that in some cases, price manipulation could lead to quasi-arbitrage, a weaker form of arbitrage, which can still destabilise the market.

While the absence of price manipulation strategies ensures regularity to some extent, it is not always sufficient. Transaction-triggered price manipulation, introduced by Alfonsi, Schied, and Slynko [1], represents a more subtle form of irregularity. It occurs when a trader can increase the expected revenues of a sell (buy) program by introducing intermediate buy (sell) trades.

Definition 2 (Transaction-Triggered Price Manipulation). *A market impact model admits transaction-triggered price manipulation if there exists an order execution strategy X_t^e , with $X_0^e > 0$, such that*

$$\mathbb{E}[\mathcal{R}_T(X^e)] > \sup \{ \mathbb{E}[\mathcal{R}_T(X)] \mid X \text{ is a monotone order execution strategy for } X_0 \text{ over } [0, T] \}.$$

Another significant form of irregularity is the existence of negative expected liquidation costs, where a trader can generate profits purely by executing a strategy, even after accounting for liquidation costs.

Definition 3 (Negative Expected Liquidation Costs). *A market impact model admits negative expected liquidation costs if there exists an order execution strategy X over $[0, T]$ such that*

$$\mathbb{E}[C_T(X)] < 0, \quad (2.4)$$

or equivalently

$$\mathbb{E}[\mathcal{R}_T(X)] > X_0 S_0. \quad (2.5)$$

For round-trip strategies, the conditions of price manipulation and negative expected liquidation costs are often equivalent. However, there are market impact models that, while avoiding price manipulation, still allow for negative expected liquidation costs. The following proposition, adapted from Klöck, Schied, and Sun [31], clarifies the relationship between these different forms of model irregularities.

Proposition 1. *1. Any market impact model that does not admit negative expected liquidation costs also does not admit price manipulation.*

2. Suppose asset prices decrease with sell orders and increase with buy orders. Then, the absence of transaction-triggered price manipulation implies that the model also does not admit negative expected liquidation costs. In particular, the absence of transaction-triggered price manipulation guarantees the absence of price manipulation in the traditional sense.

In models where such irregularities are present, traders could theoretically earn profits without taking on risk, undermining the fairness and efficiency of the market. Therefore, ensuring both regularity and the absence of irregularities like transaction-triggered price manipulation or negative expected liquidation costs is essential for maintaining the integrity of a market impact model.

2.3 Optimal Execution Strategy

The presence of market impact means we must find an optimal execution strategy to minimise adverse effects of this impact. Executing an order immediately can cause large costs due to slippage, yet executing an order fast eliminates potential uncertainty associated with future price fluctuations. Alternatively, executing the order in small increments over time may reduce immediate costs but introduces higher exposure to future price risks. As noted by [38] [38], the concept of "best execution" lacks a universally accepted definition, as it depends on both the execution costs and the potential market risks.

Financial institutions, particularly those with large positions, typically break down large orders into smaller orders to mitigate their own impact on market prices. Opti-

mal execution involves designing a dynamic strategy – a series of orders executed over a trading horizon, which adjusts according to market conditions.

To determine the best execution strategy, it is necessary to first establish a model that captures both asset price dynamics and the influence of trades on these dynamics. Then, appropriate performance criteria must be set to evaluate the effectiveness of different strategies. The ideal strategy is one that minimises execution costs while balancing risks, making it a dynamic problem with a set of constraints. We summarise the various risk criteria, which are minimised in different execution strategies, as discussed by Gatheral and Schied [22].

Mean-variance optimisation focuses on maximising a mean-variance functional of the form

$$\mathbb{E}[\mathcal{R}_T(X)] + \lambda \text{Var}(\mathcal{R}_T(X)), \quad (2.6)$$

where $\mathbb{E}[\mathcal{R}_T(X)]$ are the expected total revenue from executing a strategy X and λ is the Lagrange multiplier. Studies by [5, 4, 3, 37] have examined deterministic execution strategies under this criterion. The challenge lies in balancing trade execution costs with future price uncertainty, especially when extending these results to adverse strategies. *Expected-utility maximisation* uses a concave utility function $u : \mathbb{R} \rightarrow \mathbb{R}$, maximising the expected utility of the strategy's revenues

$$\mathbb{E}[u(\mathcal{R}_T(X))]. \quad (2.7)$$

This criterion has the advantage of time consistency, which makes it more amenable to stochastic control techniques. Schoeneborn and Schied [43] have shown that expected utility maximisation can sometimes yield solutions equivalent to mean-variance optimisation over deterministic strategies, depending on market models like the Bachelier model [6].

Expected cost minimisation focuses on minimising a functional of the form

$$\mathbb{E}\left(\sum_{t=1}^T P_t S_t\right), \quad (2.8)$$

where P_t represents the price of the asset at time t , impacted by trading, and S_t denotes the volume of the asset to be executed in the t -th trading interval. This framework was studied by Bertsimas and Lo [7], where they demonstrated that, given a block of shares to be executed within a finite time horizon T , and an impact function capturing market conditions, an optimal trading sequence exists that minimises the expected cost of executing the block of shares within T periods.

2.4 Temporary and Permanent Price Impact

The first generation of impact models makes a distinction between the following two components of impact [22, 24]. Temporary market impact, also known as execution cost, refers to the immediate price shift caused by a trade as liquidity is taken from the market. This impact only affects the trade that triggers it. In comparison, permanent market impact is a change in the asset's price that affects both the trader's current trade and all others' future trades.

These distinctions are central to execution models, particularly linear market impact models, which have been widely used to optimise trading strategies and analyse transaction costs. Linear models, such as those developed by Almgren and Chriss [4], assume a direct proportional relationship between trade size and price impact. This assumption has enabled the creation of robust tools for optimal execution, especially in addressing concerns like price manipulation and mean-field games [32].

In Almgren and Chriss' (AC) model [4] for optimal trade execution, the goal is to balance the execution cost, arising from temporary and permanent price impacts, with the volatility associated with order execution. The model determines the optimal trading strategy by minimising a combination of these two factors. The strategy is defined over a finite time horizon $[0, T]$, which is divided into N equal intervals, where N is the total number of time steps. At each time step t_j , $j = 1, \dots, N$, the trader holds a position x_j of the security. The objective is to liquidate an initial position X_0 down to zero by the end of the time period. However, this dissertation concerns itself with the problem of a trader building up a position X_0 before time T .

The price dynamics for the security follow an arithmetic random walk [5, Eqn. (1)],

$$S_j = S_{j-1} + \sigma \sqrt{\tau} \xi_j - \tau g\left(\frac{v_j}{\tau}\right), \quad (2.9)$$

where S_j represents the security's price at time t_j , $\sigma \in \mathbb{R}_+$ is the asset's volatility, and $\{\xi_j\}_{j=1}^N$ are mutually independent and follow the distribution $\xi_j \stackrel{\text{i.i.d.}}{\sim} \mathcal{N}(0, 1)$. $\tau = T/N$ denotes the time interval between trades. The function f , typically increasing and convex, models how the trading rate v_j permanently alters the price.

For temporary impact, Almgren and Chriss [5, Eqn. (2)] defined the effective execution price in each interval as

$$\tilde{S}_j = S_{j-1} - h\left(\frac{v_j}{\tau}\right), \quad (2.10)$$

where function h captures the temporary price impact caused by the trading rate in the interval $[t_{j-1}, t_j]$. The function h typically models the temporary shift in the price, which recovers after the trade is executed, and is usually a concave, increasing function

of the trading rate.

The model optimises the trade-off between execution cost and volatility risk by solving for a strategy that minimises a quadratic utility function, or by minimising the expected shortfall with a constraint on the variance, as defined in Equation (2.6).

Following Coxon [16, Section 1.3.2], we choose $g(x) = \gamma x$ and $h(x) = \epsilon \text{sgn}(x) + \eta x$, where γ represents the rate of permanent impact and $\epsilon > 0$ is a constant factor representing the fixed component of the temporary price impact. Then we optimise the mean variance problem with coefficient λ , and obtain the optimal trading strategy under the AC model in the limit of $\tau \rightarrow 0$

$$x_j = X_0 \left(1 - \frac{\sinh(\kappa(T - t_j))}{\sinh(\kappa T)} \right), \quad j = 0, \dots, N, \quad (2.11)$$

where $\kappa = \sqrt{\lambda \sigma^2 / \eta}$ is the risk aversion parameter, and σ and η are volatility and liquidity parameters, respectively. As $\kappa \rightarrow 0$, the trader is less risk-averse, and it will execute the position at a steady, linear rate through the trading period T . As κ grows large, reflecting a risk-averse trader, the strategy prioritises immediate execution to minimise exposure to future market risk. The trading trajectory becomes front-loaded, meaning that the bulk of the trade is executed early in the trading window. The strategy approaches instantaneous execution of the entire position, regardless of the cost of immediate market impact. It is suited for volatile market conditions.

2.5 Transient Price Impact

An alternative perspective suggests that trades cause temporary price shifts rather than permanent changes, preserving market efficiency. Permanent price impacts would distort market dynamics by allowing trades to cause lasting disruptions, preventing prices from reflecting true supply and demand. As liquidity replenishes, the impact of a trade diminishes, allowing prices to revert to equilibrium. This transient impact prevents long-lasting autocorrelations in returns, consistent with empirical evidence that price movements should not have persistent effects [11]. This highlights the need to model price impact as transient, capturing its decaying nature.

One approach to modelling this is through the Transient Impact Model (TIM), which focuses on how the impact of trades decays over time. In TIM, the impact from an executed trade gradually fades as liquidity replenishes, and prices return to their pre-trade equilibrium.

The transient impact of trades can be modelled using the price impact kernel $G: \mathbb{R}_+ \rightarrow \mathbb{R}$, also known as the propagator. This kernel quantifies how the impact of a trade diminishes over time, determining whether the system exhibits Markovian or non-Markovian behaviour.

2.5.1 General Transient Impact Model

The total price impact in a general transient model is given by

$$S_t^X = S_0 + \int_0^t G(t-s) dX_s + M_t, \quad (2.12)$$

where S_t is the impacted price, S_0 is the unaffected price, dX_s is the trading volume at time s , and M_t is a martingale representing random market fluctuations.

In the deterministic setting, Gatheral and Schied [23] shows that, *without* signals and risk-aversion terms, the optimal trading strategy can be obtained by minimising an energy functional under the assumption that the kernel G is non-increasing, convex, and integrable. This leads to solutions based on Fredholm-type equations, which were further extended by Alfonsi, Schied, and Slynko [1] to include infinite-dimensional Riccati equations.

However, when signals are introduced, the strategies become signal-adaptive. Such adaptive strategies respond dynamically to incoming market data, such as order book dynamics, creating more complex trading paths that require advanced stochastic control tools, like backward stochastic differential equations. They are thus no longer deterministic [41].

2.5.2 Linear Transient Impact: Obizhaeva-Wang Model

The Obizhaeva-Wang (OW) model [42] is an example of transient price impact modelling, particularly suited for optimal execution problems in a LOB setting. It assumes that large market orders temporarily deplete liquidity, raising prices, and that this price impact decays over time as new limit orders replenish the book. The decay is governed by an exponential resilience factor $\rho \in \mathbb{R}_+$, representing the speed at which liquidity recovers. This exponential propagator renders the liquidation problem Markovian, as the transient price impact can be regarded as a mean-reverting state variable [30].

The evolution of the ask price due to a trade is given by Obizhaeva and Wang [42] as

$$a_t = S_0 + \lambda_{\text{OW}} v_0 + \frac{s}{2} + v_0 \kappa e^{-\rho t}, \quad (2.13)$$

$$\kappa = \frac{1}{q} - \lambda_{\text{OW}}, \quad (2.14)$$

where s is the bid-ask spread, λ_{OW} represents permanent price impact, and q is the LOB density, or market depth. Higher market depth reduces price sensitivity to large trades, as more shares are available near the current price. A shallow market depth,

on the other hand, leads to greater price sensitivity and larger price impacts.

The OW model does not take into account trading signals, resulting in deterministic optimal strategies. This sets it apart from more complex models where strategies adapt dynamically to market signals, introducing non-Markovian dynamics [30]. Without signals, the model remains tractable and well-suited for scenarios where adaptability is less critical.

The cost minimisation problem for executing X_0 shares over time is formulated as

$$\begin{aligned} \min_{\{v_0, v_1, \dots, v_N\}} \mathbb{E} & \left[\sum_{j=0}^N \left(S_j + \frac{s}{2} + \sum_{i=0}^{j-1} \left(\lambda_{\text{OW}} v_i + v_i \kappa e^{-\rho \tau(j-i)} \right) + \frac{v_j^2}{2q} \right) v_j \right] \\ \text{s.t.} \quad & \sum_{j=0}^N v_j = X_0, \end{aligned} \quad (2.15)$$

where v_0 is the initial trade size, and v_j is the volume traded at time t_j , $j = 0, \dots, N$. This objective function captures both immediate impact through $\lambda_{\text{OW}} v_i$ and decayed impact via $v_i \kappa e^{-\rho \tau(j-i)}$, balancing execution costs over time.

Despite sacrificing some accuracy compared to models with slower decaying, power-law kernels, the OW model's exponential decay assumption simplifies the problem, providing clear, analytically tractable solutions for deterministic strategies.

In the study of transient price impact models, a result by Gatheral and Schied [23] offered conditions for ensuring the regularity of market impact models. Proposition 2 from Gatheral and Schied [23] linked the positivity of the decay kernel G and the absence of price manipulation and negative expected liquidation costs. This feature, further supported by Alfonsi, Schied, and Slynko [1], ensures that optimal execution strategies remain monotonic.

Proposition 2. *Suppose that G is continuous and finite. Then the following are equivalent:*

1. *The model does not admit negative expected liquidation costs.*
2. *G is positive definite in the sense of Bochner [8].*
3. *$G(|\cdot|)$ is the Fourier transform of a nonnegative finite Borel measure on \mathbb{R} .*

In particular, the model does not admit price manipulation when these equivalent conditions are satisfied.

2.6 Limitations of the Transient Impact Model

One of the primary limitations of the TIM is that it can become inconsistent under certain conditions, particularly when non-linear impact functions are used. The impact function $f : \mathbb{R} \rightarrow \mathbb{R}$, which models how price impact scales with trading speed,

is central to the model's dynamics. When this function is non-linear, TIMs risk violating key no-arbitrage conditions, leading to price manipulation. Empirical evidence consistently demonstrates that price impact depends on trade size in a concave, non-linear manner, whether estimated from proprietary trade data or public market data. For example, studies by [35, 25, 26, 9, 2, 21, 20] all confirm this concave relationship across various datasets.

Gatheral and Schied [23] demonstrated that when the impact function is non-linear, such as $f(v) \propto v^\delta$, where $\delta \in \mathbb{R}_+$ is the exponent, combined with an exponential decay kernel $G(t-s) = e^{-\rho(t-s)}$, the model becomes prone to price manipulation. In this context, t represents the current time and s denotes a past trade time, where $0 \leq s < t$. The non-linearity in the impact function, together with the exponential decay, allows for dynamic arbitrage, where traders can exploit the model's inconsistencies. By executing a series of trades that generate profits and returning to their original position without incurring any cost, traders would contradict realistic market behavior. To maintain consistency and prevent price manipulation, TIMs typically require the impact function to remain linear, ensuring that such arbitrage opportunities do not arise.

Power-law decay has been proposed as an alternative to exponential decay because it more accurately reflects real-world market dynamics. However, even with power-law decay, price manipulation can still occur if the non-linear function f does not satisfy certain conditions. Specifically, the no-dynamic-arbitrage condition requires that

$$\rho + \delta \leq 1, \tag{2.16}$$

This constraint ensures that the model is consistent and prevents arbitrage. As a result, this condition imposes limitations on the permissible values of ρ and δ , which may reduce the model's ability to describe market behaviour accurately.

2.7 Moving Towards the Discrete Propagator Model

Given the limitations of the TIM, the DPM offers an alternative discrete time formulation. This aligns closely with the actual execution of trades. In the DPM, each individual trade has a distinct, measurable impact on the market, which allows for greater granularity in capturing how market impact propagates. This is especially important in environments where trades are executed at irregular intervals and the precise effect of each trade needs to be modelled separately, as supported by the work of Bouchaud et al. [9] and recent studies by Muhle-Karbe, Wang, and Webster [39].

We focus on a financial market with a risky asset. Its fundamental price is modelled using a continuous semimartingale S , which represents price fluctuations caused by exogenous factors like news, rather than by trading activities. Additionally, another

continuous semimartingale F captures the signed order-flow. The impact state model $I = I(F)$ describes how this order-flow F influences the actual market price $S + I$, at which trades are executed, relative to its fundamental value S [39].

Definition 4. *At the microstructure level, the price impact has the dynamics*

$$\Delta I_n = -\beta I_{n-1} \Delta t + f(\Delta F_n), \quad (2.17)$$

for $\beta > 0$ and some odd and continuously differentiable function f that is concave on $[0, \infty)$. $\Delta I_n = I_n - I_{n-1}$ denotes the change in impact state over the discrete time interval $[t_{n-1}, t_n)$, ΔF_n represents the signed trading volume in the same interval, and f remains the impact function.

The term $-\beta I_{n-1} \Delta t$ serves as a decay mechanism, allowing the market impact to dissipate over time. The parameter β , known as the decay parameter, controls the rate at which past impacts diminish. It serves the same role as ρ in earlier sections but follows the notation from Muhle-Karbe, Wang, and Webster [39] for consistency. It is inversely related to the impact state's half-life, defined as the time it takes for the impact state's magnitude to reduce by half. The half-life is given by $\text{half-life} = \ln 2 / \beta$. A larger β corresponds to a shorter half-life, resulting in faster decay of past impacts, while a smaller β leads to slower dissipation of impact over time.

As the function f is odd, the price impact for purchases and sales is symmetric, and its concavity ensures that trading twice the volume does not result in twice the price impact. In the simplest case, where $f(v) = \lambda v$, the model corresponds to the OW.

At this point, we formally introduce λ , a key parameter in price impact models. Historically, λ was first introduced by Kyle [33] as a measure of market illiquidity, representing the sensitivity of prices to order flow. In Kyle's framework, λ captured how much the price moves in response to a unit of volume traded, with higher λ values indicating that even small trades significantly affect the price. It is known as Kyle's lambda. This concept of illiquidity is central to understanding how market depth and liquidity affect trading costs, as more illiquid markets (i.e., those with higher λ) experience larger price impacts for similar trade sizes. Illiquidity is, therefore, the inverse measure of liquidity – where more liquid markets exhibit smaller price impacts for equivalent trades. In the context of more recent models like the OW, λ_{OW} served as the permanent price impact coefficient. It governs the magnitude of the price shift that persists after a trade, reflecting how much of the impact is irreversible and embedded in the market price. By incorporating λ_{OW} , the OW model and similar frameworks quantify the long-lasting effects of trades, distinguishing between transient price fluctuations and those that represent a permanent shift in market prices.

In the DPM, λ captures the illiquidity of an asset. As trades accumulate over time, the presence of λ ensures that each trade's impact is factored into both immediate and decayed price changes. From this point forward, λ is the illiquidity parameter. The DPM extends the OW by allowing for non-linear impact functions, better capturing the concave nature of real-world price impacts observed in empirical studies [9].

Muhle-Karbe, Wang, and Webster [39] introduced this framework for modelling non-linear price impacts in discrete time, allowing for a more granular approach to capturing how trades influence market prices. This structure aligns with the reality of financial markets, where trades occur discretely, and price impact propagates in a time-dependent fashion.

The shape of the function f at the microstructure level has been a focal point in various studies. Muhle-Karbe, Wang, and Webster [39] have highlighted several key findings.

In the original propagator model by Bouchaud et al. [9], the impact function takes the form $f(v) \propto \log(v)$.

Bouchaud, Farmer, and Lillo [10] reviewed empirical evidence indicating that price impact often follows a power-law behavior, where $f(v) \propto v^p$ with exponents $p \in [0.2, 0.5]$.

Bucci [13] documented a crossover between different impact regimes. For small trades, the impact is linear, $f(v) \propto v$, while for larger trades, the impact transitions to a square-root law, $f(v) \propto v^{1/2}$.

These distinct forms of f offer flexibility to accurately capture varying market behaviors, reflecting how the impact scales with the size of the trade [39].

We now turn to the methodology and results of parameter estimation for the DPM, following the approach of Muhle-Karbe, Wang, and Webster [39]. Early studies, such as Hasbrouck [25], laid the foundation for propagator models by regressing price changes on lagged values of order-flow. Building on this, Muhle-Karbe, Wang, and Webster [39] calibrated the DPM using constituent stocks of the S&P 500, regressing horizon-specific returns onto impact returns. The two key concepts are defined as follows.

- **Horizon-specific return:** The mid-price return over a horizon h starting at time t is defined as

$$\Delta_t^h P = \frac{P_{t+h} - P_t}{P_t}, \quad (2.18)$$

where P_t and P_{t+h} are the mid-prices at time t and $t+h$, respectively.

- **Horizon-specific impact return:** The impact return, or change in impact state over a horizon h starting at time t , incorporating both the immediate order-flow

and the decay of past impacts, is

$$\Delta_t^h I = I_{t+h} - I_t, \quad (2.19)$$

where I_t and I_{t+h} are the impact states at time t and $t + h$, respectively.

The horizon h can represent the length of prediction intervals, and has to be a multiple of the time bin duration picked for aggregation.

The regressions performed to estimate the DPM parameters follow the form

$$\Delta^h P = \Delta^h I + \varepsilon, \quad (2.20)$$

where $\Delta^h I$ depends linearly on λ across the parametric models. This setup provides a clear mechanism for fitting the magnitude of price impact by adjusting λ within the parametric model choice [39]. Empirically, it is observed that the prediction power of price impact models decreases as the prediction horizon h increases. The predictive accuracy of a model is typically measured by the coefficient of determination, denoted as R^2 . This metric represents the proportion of the variance in the dependent that is predictable from the independent variables. In the context of price impact models, a higher R^2 indicates a stronger ability of the model to explain the variation in price movements caused by trading volumes. or short horizons, such as 1 minute, the concave propagator model, where $f(v) \propto v^{1/2}$, significantly outperforms the linear OW model $f(v) \propto v$, achieving an out-of-sample R^2 of 18%, compared to 10% for the OW model. As the horizon increases (e.g., 15 and 60 minutes), the predictive power diminishes for both models, with longer horizons leading to weaker R^2 values.

The incorporation of a time-dependent illiquidity parameter adds flexibility to the model by accounting for liquidity fluctuations throughout the trading day. In this framework, λ is re-fit on an hourly basis, creating a time-dependent illiquidity time series λ_t , where t denotes the specific hour within the trading day. This allows λ_t to adapt to changing market conditions. The hourly re-fitting reduces residual errors that arise from assuming constant liquidity, especially when employing a concave propagator model with a square-root impact function [39]. These results highlight the advantages of a time-dependent illiquidity parameter and concave impact functions when modelling price impact over short prediction horizons, where market activity is particularly sensitive to liquidity variations.

2.8 The Bitcoin Market

Bitcoin, created by Nakamoto [40], was designed as a decentralised cryptocurrency to enable transactions without the need for a central authority. Since its inception,

Bitcoin has grown in market capitalisation, reaching billions of dollars by 2013. In this study, Bitcoin refers to the cryptocurrency and protocol, while BTC will be used specifically to denote the unit of currency in transactions and trading volumes. A BTC unit is divisible into 100 million smaller units called satoshis, which allows for fractional trading volumes. While Bitcoin is traded on organised exchanges similar to traditional financial assets, its market microstructure displays unique features, particularly concerning liquidity and intraday trading patterns, which distinguish it from conventional equity and currency markets.

Bitcoin's intraday trading behaviour is shaped by its global and continuous nature. Several studies have examined the distinct intraday dynamics, especially regarding how liquidity, trading volume, and volatility evolve over the course of the day. Wang, Liu, and Hsu [46] analysed Bitcoin's intraday periodicities and show that trading volume follows a reverse V-shaped pattern, peaking during European and US stock market hours, with a noticeable drop during periods when these markets are closed. This aligns Bitcoin's most active trading hours with those of traditional financial markets, similar to foreign exchange, where activity intensifies at the opening and closing of major stock exchanges.

Further research by Eross et al. [19] complemented these findings by demonstrating that Bitcoin's liquidity fluctuates throughout the day, with the highest levels observed during the overlap of European and US market hours. Despite Bitcoin's 24/7 trading framework, liquidity conditions are heavily influenced by traditional market participants, as shown by the drop in liquidity during the early morning hours when major global markets are closed. This reflects the interplay between retail and institutional investors in Bitcoin, with trading activity coinciding with broader financial market movements. Notably, Wang, Liu, and Hsu [46] argued that traditional liquidity measures, such as Kyle's lambda, remain robust in the context of cryptocurrency markets, serving as a reliable indicator of liquidity risk in Bitcoin.

3 Data Preparation

3.1 Motivation

As discussed in Section 2.7, we aim to calibrate a DPM on the exchange rate BTC/USD. While many studies have applied propagator models to traditional financial markets, relatively few have explored their use on cryptocurrency data. The DPM offers a robust framework for capturing non-linear market impact, particularly with the impact exponent 0.5 [39]. The OW model, which assumes an impact exponent of 1 and constant parameters, has been well studied, but its assumption of linear impact is a limitation when applied to the cryptocurrency market. Our approach is to focus on a range of impact exponents from 0.10 to 0.70, reflecting the findings of Bouchaud, Farmer, and Lillo [10], who demonstrated that market impact behaves as a strongly concave function at shorter time scales but tends to become more linear over longer horizons. This choice allows us to explore the full spectrum of potential non-linearity in Bitcoin’s market impact, capturing both the short-term concave behavior and the more linear patterns over extended periods. To effectively calibrate these impact models, it is essential to work with normalised and binned data. This ensures that the findings of the DPM can be universally compared across assets [39].

3.2 Tardis Data

This dissertation uses Tardis, as its data source of granular data provider for cryptocurrency markets [45] that offers access to high-frequency, tick-level data for both spot and derivative cryptocurrency exchanges. Tardis supplies comprehensive datasets, including tick-by-tick trade information (such as price, volume, and the buy/sell direction) alongside order book snapshots, which include best bid and ask quotes and their respective sizes. These order book snapshots are updated with each incoming message to the order book, including events such as order submissions, cancellations, modifications, or executions. The dataset spans a wide variety of exchanges, including Kraken, Binance, and Coinbase, and supports the full reconstruction of the LOB for both historical and real-time data.

The focus of this study is a dataset spanning four months, from May 5, 2024, to September 3, 2024. This dataset comprises daily data for both trades and quotes. Table 1 provides an overview of the structure of the dataset, which includes 82.7 million individual quote snapshots and 3.3 million trades. The trades and quotes are stored separately. The quotes, given their higher frequency, make up the bulk of the dataset.

The dataset distinguishes between trades and quotes, with traded volumes ex-

Column Name	Data Type	Description
timestamp	int64	Timestamp in microseconds.
exchange	string	Exchange name (Kraken).
symbol	string	Trading pair.
side	string	Trade direction, 'buy' or 'sell'.
price	float32	Trade execution price.
amount	float32	Traded volume
ask_amount	float32	Volume at the ask price.
ask_price	float32	Current ask price.
bid_price	float32	Current bid price.
bid_amount	float32	Volume at the bid price.

Table 1: Kraken trades-and-quotes file formats.

pressed in BTC and the bid and ask prices in US dollars (USD). Volumes at the best bid and ask prices are also recorded in BTC. The trading pair, or exchange rate, used throughout this study is BTC/USD.

In trades-and-quotes datasets, there is a direct correspondence between the transaction price at time t , denoted as p_t , and either the best ask or bid price, represented as a_t or b_t , respectively. A transaction at $p_t = a_t$ indicates a buy market order (with an order sign $\epsilon_t = +1$), while a transaction at $p_t = b_t$ indicates a sell market order (with an order sign $\epsilon_t = -1$). Each data entry also includes the trade volume at time t , v_t . When the buy or sell market order is smaller than the available volume at the best ask or bid, v_t captures the full order size. If the market order volume exceeds the available volume at the best ask or bid, the remaining portion is executed at subsequent prices, and transaction costs arise based on the size and price of the market order. Any unfilled portion is added to the limit order book at the submitted price. Such activities are typically recorded as distinct, consecutive transactions with the same or nearly identical timestamps in trades-and-quotes datasets [11, Chapter 11].

A key assumption in our analysis is that most trades recorded in the dataset are market orders, as they represent trades that are executed immediately. While various forms of order-flow – such as market orders, limit orders, and cancellations – contribute to price movements, the immediate focus of this study is on market orders due to their direct impact on price discovery. This approach aligns with the work of Bouchaud et al. [11, Chapter 11], where market orders were identified as primary drivers of price impact in trades-and-quotes datasets.

A significant quantity in price impact modelling is the signed trade volume. Unlike previous studies that infer trade initiation (buy or sell) from price movements, our dataset explicitly marks whether the buyer or seller initiated each trade, thus eliminating the need for inference methods such as the tick rule, which are commonly used but error-prone for small trades [16]. As outlined by Holthausen, Leftwich, and Mayers

[28, Table 4], such inference methods struggle to classify trades with smaller volumes, which can introduce biases in volume estimation.

For the purpose of our study, v_t is multiplied by -1 for sell-initiated trades. We aggregate this signed volume over a given time bin,

$$\Delta F_n = \sum_{t_{n-1} < t \leq t_n} \epsilon_t v_t, \quad (3.1)$$

where t_{n-1} is the start time of the bin and t_n is the end time of the bin.

In constructing the dataset for model calibration, time can be measured either in "market-order time" (incremented by 1 for each market order arrival) or in real calendar time. Following the methods used by Cont, Kukanov, and Stoikov [15], we opt for the latter, with 10-second bins aggregating trades and quotes over each trading day. This approach results in 8,640 bins per 24-hour period. However, as noted by Coxon [16], binning reduces observed absolute volume. For example, two opposing trades of the same magnitude within a time bin may cancel each other out, yielding a net zero net signed volume for that bin. This could obscure trends and periodicities in intraday volume. To ensure this effect does not affect our analysis, we follow the methodology of Coxon [16, Subsection 3.2], comparing the total volume and the absolute value of net signed volume to observe how aggregating signed volume affects intraday patterns:

- Total volume $\sum_{t_{n-1} < t \leq t_n} v_t$, representing the overall volume traded within the bin, irrespective of whether trades were buy- or sell-initiated.
- Absolute of net signed volume $|\Delta F_n|$, capturing the magnitude of the net effect of buy- and sell-initiated trades, ensuring non-negative values.

By plotting these measures in Figure 1, we can assess whether aggregating signed volume significantly affects the visibility of intraday trading trends, such as peaks and troughs in trading activity.

The bottom plot shows that when total volume is high within a given 15-minute time bin, the trade signs tend to be correlated, resulting in minimal reduction of volume from opposite-sign trades. However, values for net signed volume can still be relatively low compared to peak values of total volume, indicating that buy- and sell-initiated trades offset each other to some extent. In cases where $\sum_{t_{n-1} < t \leq t_n} v_t$ is smaller, the volumes of buy- and sell-initiated trades may cancel each other out completely. Nonetheless, we are confident that both time series are sufficiently correlated to justify their use in our analysis.

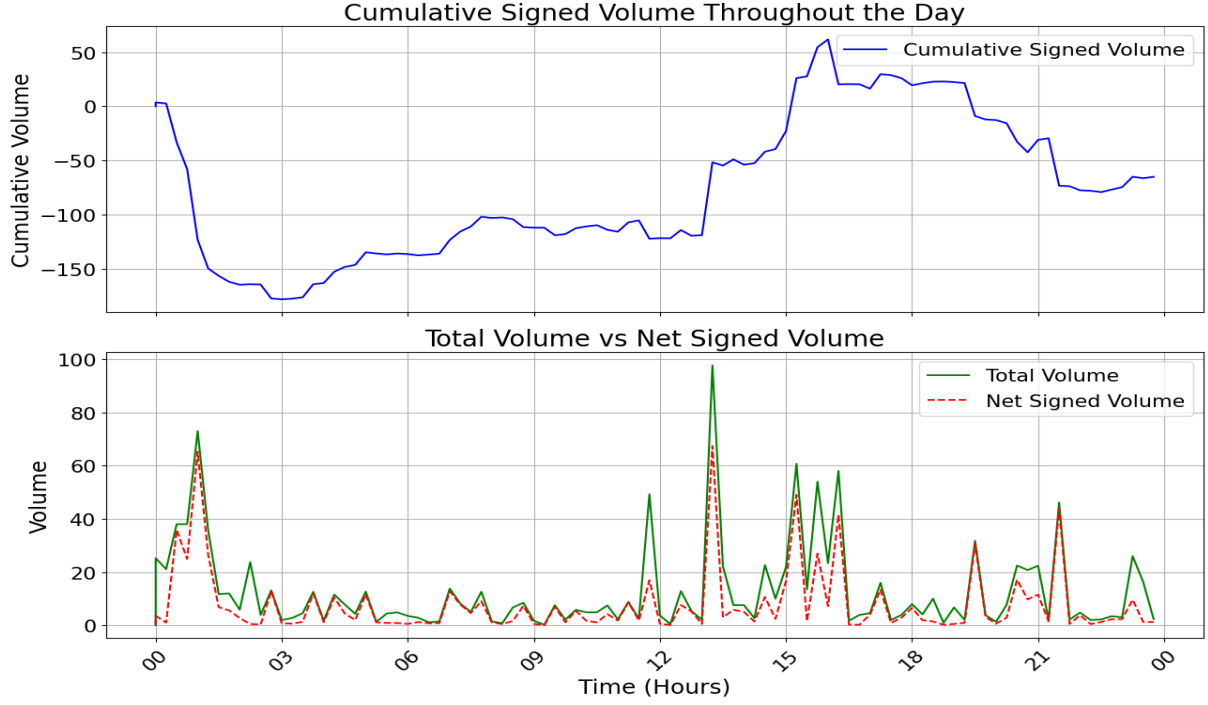


Figure 1: Plot of cumulative signed volume throughout the day (top) and plot of total volume $\sum_{t_{n-1} < t \leq t_n} v_t$ vs. absolute of net signed volume $|\Delta F_n|$ (bottom) for the 2024-05-05 trading day. Both plots use 15-minute bins for better visualisation.

3.3 Data Normalisation

As established in Section 2.1, price impact refers to the expected price change conditional on the execution of a trade of a given size and direction. When modelling price impact, it is essential to carefully define the units in which these price changes are measured. In foundational models, such as the AC model [4], price changes were modelled in terms of the absolute price of the asset. Conversely, other models, such as [14, 34], use the log price of the asset to better capture the relative changes in price over time. Furthermore, in more recent work by Muhle-Karbe, Wang, and Webster [39], $\Delta_t^h I$ was regressed against $\Delta^h P$, thereby normalising the impact return as a function of mid-price returns. Additionally, Hey et al. [27, Section 4.1] and Muhle-Karbe, Wang, and Webster [39, Section 5.2] applied normalisation procedures in which the traded volume, ΔF , is divided by the rolling average daily volume (ADV), and the price impact is normalised by multiplying it by the rolling daily σ . These normalisations are fundamental for ensuring consistency and comparability across different assets. As Muhle-Karbe, Wang, and Webster [39] has highlighted, normalising using both σ and the ADV is essential to achieve stable and comparable estimates of λ across various stocks. Without such normalisation, the universal price impact models would not produce a stable λ , making direct comparisons with stock-specific models infeasible. Two key functions are introduced to account for both volume and volatility: the

simple moving average (SMA) of the daily trading volume over the preceding k days on day m ,

$$V_{\text{avg}}(m, k) = \frac{1}{k} \sum_{j=1}^k v_{m-j}, \quad (3.2)$$

where v_i represents the traded volume on day i , and the SMA of the daily mean standard deviation of the 10-second mid-price returns over the same period,

$$\sigma_{\text{ret}}(m, k) = \frac{1}{k} \sum_{j=1}^k \sigma_{m-j}, \quad (3.3)$$

where σ_i denotes the mean standard deviation of the 10-second mid-price returns on day i .

Using the relationship $\Delta I_n^m = I_n^m - I_{n-1}^m$ as defined in Definition 4 and generalised to be within day m , the model transformation after normalisation is expressed as

$$\frac{\Delta I_n^m}{\sigma_{\text{ret}}(m, k)} = -\beta \Delta t \frac{I_{n-1}^m}{\sigma_{\text{ret}}(m, k)} + f\left(\frac{\Delta F_n^m}{V_{\text{avg}}(m, k)}\right), \quad (3.4)$$

which simplifies to

$$\Delta I_n^m = -\beta \Delta t I_{n-1}^m + \sigma_{\text{ret}}(m, k) f\left(\frac{\Delta F_n^m}{V_{\text{avg}}(m, k)}\right). \quad (3.5)$$

Here, ΔI_n^m and ΔF_n^m denote the impact state and signed trading volume, respectively, for day m , at time t_n . I_{n-1}^m represents the impact state at the previous time t_{n-1} , within the same day m . I_{n-1}^m accounts for the cumulative effect of past trades up to time t_{n-1} , which decays over time as governed by G .

The normalisation functions ensure consistency across different assets and follow the principles outlined by [2, 16]. They dynamically adjust for both volume and volatility over a lookback period k , where $k = 30$ to represent a rolling average over one month of trading. This ensures that the most recent market conditions are reflected.

These normalisations give rise to the updated expression for the DPM, which is used to calibrate it to public trading data for BTC/USD exchange rate,

$$\Delta I_n^m = -\beta \Delta t I_{n-1}^m + \sigma_{\text{ret}}(m, 30) f\left(\frac{\Delta F_n^m}{V_{\text{avg}}(m, 30)}\right), \quad (3.6)$$

where n represents the indices of 10-second time bins within day m .

As shown in Figure 2, Equation (3.2) and Equation (3.3) smooth out the daily trading volume and the standard deviation of binned returns, respectively.

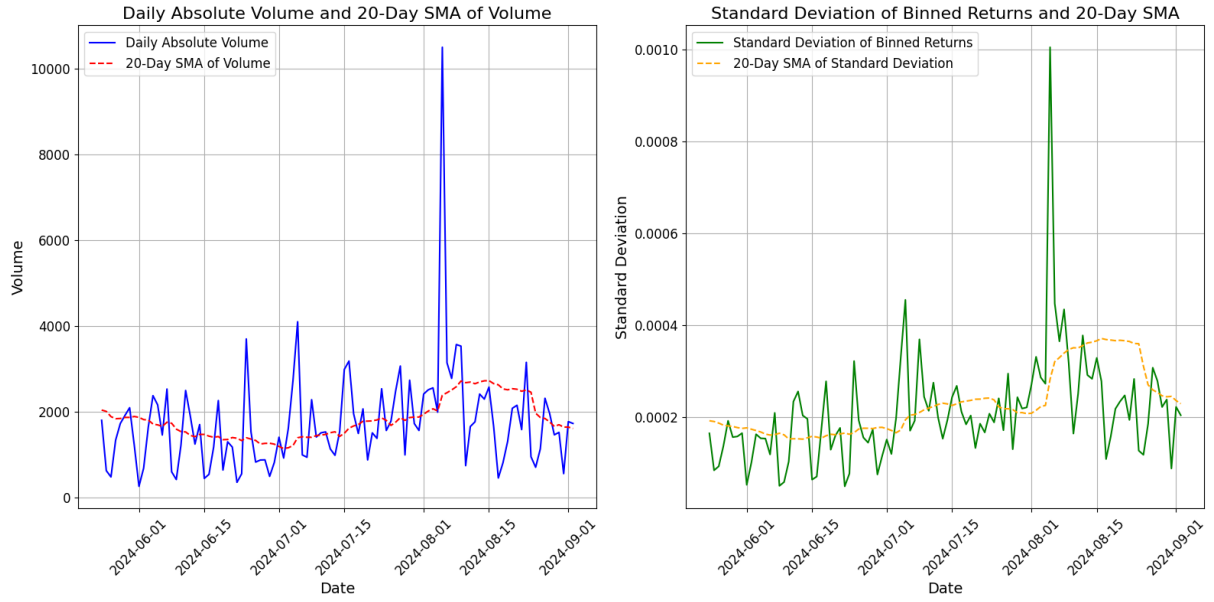


Figure 2: Comparison of daily volume with the 30-day SMA of volume, calculated using $V_{avg}(m,k)$ (left), and comparison of σ with the 30-Day SMA of standard deviations of binned return, calculated using $\sigma_{ret}(m,k)$ (right).

4 Model Calibration

The underlying methodology for calibrating the DPM is derived from open source code by [17].

4.1 Methodology

As outlined in Section 3.3, we calibrate the model for the change in impact according to

$$\Delta I_n^m = -\beta \Delta t I_{n-1}^m + \sigma_{\text{ret}}(m, 30) f\left(\frac{\Delta F_n^m}{V_{\text{avg}}(m, 30)}\right), \quad (4.1)$$

where we assume a functional form of $f(v) = \lambda \text{sgn}(v)|v|^\delta$. To illustrate the dependency of the change in impact on the parameters, we have

$$\Delta I_n^m = \Delta I_n^m(\lambda, \delta, \beta) = -\beta \Delta t I_{n-1}^m + \sigma_{\text{ret}}(m, 30) \lambda \text{sgn}\left(\frac{\Delta F_n}{V_{\text{avg}}(m, 30)}\right) \left|\frac{\Delta F_n}{V_{\text{avg}}(m, 30)}\right|^\delta. \quad (4.2)$$

We use the relationship defined in Equation (2.20) to assume that $\Delta^h P$ corresponds to the expected value of $\Delta^h I_n(\lambda, \delta, \beta)$, plus a random error term $\epsilon \sim \mathcal{N}(0, \sigma^2)$,

$$\Delta^h P_n(\lambda, \delta, \beta) = \Delta^h I_n(\lambda, \delta, \beta) + \epsilon. \quad (4.3)$$

The impact dynamics are influenced by the choice of decay kernel G . For simplicity and tractability, we adopt the exponential form of G , as used in Obizhaeva and Wang [42]. This choice ensures that the problem remains Markovian, with the system depending solely on its current state.

The exponential decay reflects the diminishing influence of past trades, governed by the decay parameter β . The impact from past trades decreases exponentially, following the update rule

$$I_n^m = (1 - \beta h) I_{n-1}^m + \sigma_{\text{ret}}(m, 30) g\left(\frac{\Delta F_n^m}{V_{\text{avg}}(m, 30)}\right). \quad (4.4)$$

The term $1 - \beta h$ scales the previous impact state, while $f(\Delta F_n^m / V_{\text{avg}}(m, 30))$ captures the effect of the latest traded volume. Following the approach in Cont, Kukanov, and Stoikov [15], we set the prediction horizon h to match the duration of a single time bin, $\Delta t = 10$ seconds. This makes the model explanatory, as it describes price changes over the same interval in which the volume is traded.

The next step involves assigning fixed values β and λ . We choose arbitrarily a value $\beta = 0.7$, in line with the findings and methods of Muhle-Karbe, Wang, and Web-

ster [39], which corresponds to a one hour half-life in hourly units. A baseline value of $\lambda = 1$ is assumed to decouple the impact's functional form from its scale. This allows us to express $\Delta I_n(\lambda, \delta, \beta)$ as $\lambda \Delta I_n(1, \delta, \beta)$.

The concavity of the price impact function, controlled by δ , is explored across values $\delta \in \{0.10, 0.15, \dots, 0.70\}$, similar to the approach in Coxon [16].

For each 10-second bin within an hour, we pre-compute the impact state $\Delta^h I(1, \delta, \beta)$ and regress the observed price change $\Delta^h P$ onto this computed impact state. For each δ , we estimate the parameters of the price impact model by running the regression

$$\Delta P_n(\lambda) = \Delta^h I_n(\lambda) + \epsilon \quad (4.5)$$

over the parameter choice λ . The superscript h can be dropped in Equation (4.5) as we have fixed its duration.

By repeating this process across all 10-second bins within each hour, we obtain an hourly estimate of λ . These hourly regressions are averaged across all trading days in the training period to account for time-dependent variations in illiquidity throughout the day.

Cross-validation is implemented using a sliding window approach. We use a 7-day training period and a 3-day testing period to ensure robust parameter estimates. This method allows the model to capture both long-term trends and recent market changes, providing a comprehensive evaluation of its performance.

4.2 Calibration Results

4.2.1 Observations

Table 2 summarises the key metrics derived from applying the DPM to the BTC/USD exchange rate on Kraken. The analysis covers a 3-day test period starting on 2024-06-04, with each row corresponding to an hourly segment of the 24-hour trading cycle. This allows us to capture time-dependent variations in λ_t , where t represents the specific hour of the day, $t \in \{0, 1, \dots, 23\}$, within the 24-hour trading cycle. The table reports estimates of λ_t values, alongside the corresponding R^2 scores for both the training and testing phases.

The method involves determining the optimal δ by selecting the highest mean in-sample (training) R^2 score over a 7-day training period. The corresponding λ_t values for each hour are retrieved.

Figure 3 illustrates the model's performance by plotting the R^2 scores for both training and testing periods on the left y-axis, alongside the corresponding λ_t values on the right y-axis. The model fits λ_t values to account for illiquidity variations, while

Hour	λ	Train R^2	Test R^2
0	0.35	0.03	0.02
1	4.77	0.03	0.01
2	0.39	0.03	0.02
3	0.50	0.04	0.04
4	4.38	0.03	0.04
5	4.35	0.04	0.00
6	0.37	0.03	0.05
7	0.53	0.04	-0.02
8	0.54	0.05	0.03
9	0.51	0.05	0.03
10	0.56	0.06	-0.06
11	0.48	0.04	0.02
12	0.70	0.04	0.04
13	0.63	0.03	0.03
14	0.79	0.05	0.03
15	0.63	0.04	0.02
16	0.48	0.03	0.03
17	0.42	0.03	0.01
18	0.41	0.03	0.02
19	5.35	0.04	0.03
20	3.57	0.02	0.03
21	4.00	0.04	0.02
22	2.52	0.02	0.03
23	0.29	0.02	0.03

Table 2: Hourly λ_t values with corresponding train R^2 and test R^2 using 7 days of training followed by 3 sequential days of testing for $\delta = 0.1$. The train period ends on June 04, 2024.

the test R^2 scores are based on the 3-day testing period following each training window. This process is repeated for several end-of-training dates.

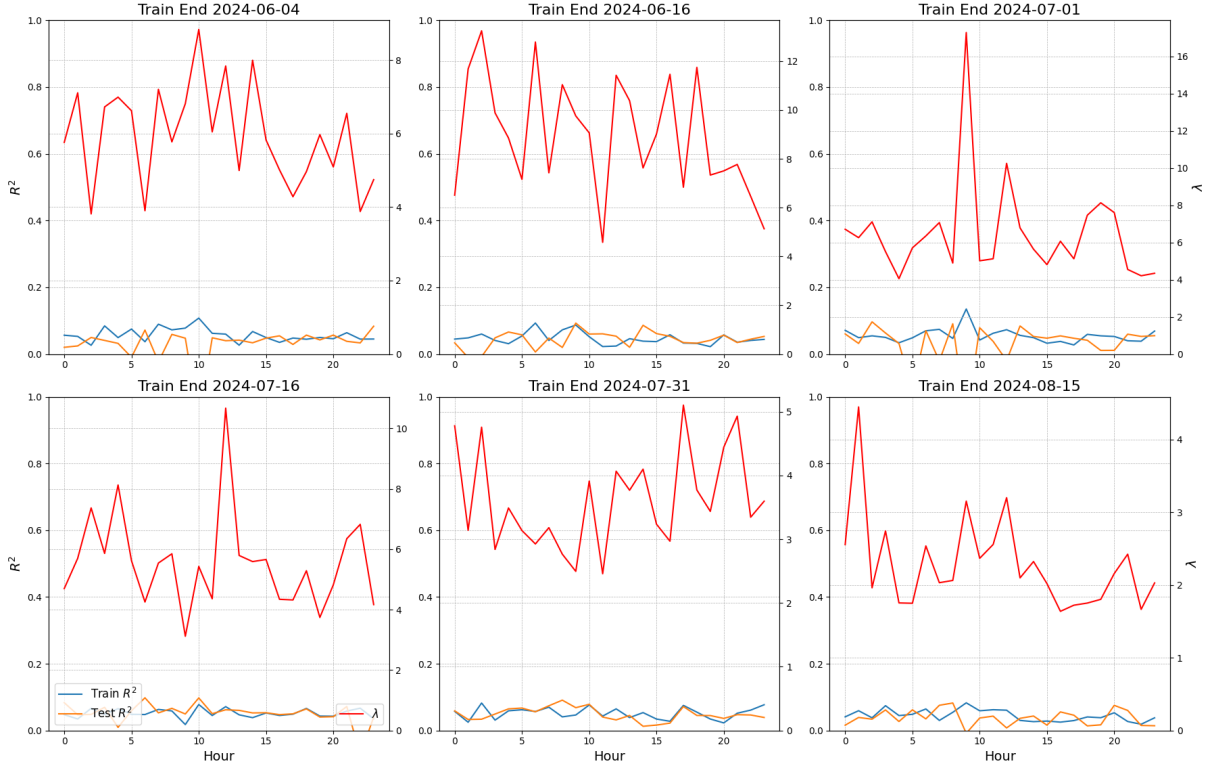


Figure 3: Visualisation of the intraday training and testing R^2 scores alongside the corresponding intraday λ_t values for various end-of-training dates, and using the optimal exponent $\delta = 0.35$. Training period is 7 days, testing period is 3 days. The UTC time-zone is used throughout the analysis [45].

The λ_t values exhibit significant fluctuations throughout the day. Notably, large λ_t values tend to appear during the early hours of the trading day (e.g., 1:00 AM, 4:00 AM, and 5:00 AM), potentially coinciding with lower liquidity during Asian and European trading hours. As global market activity picks up, particularly when European and US markets overlap, the λ_t values stabilize. This aligns with findings in the literature that Bitcoin’s liquidity is highly influenced by traditional financial market hours, as discussed in [46, 19].

The plots in Figure 3 reveal low R^2 values, which hover around 5%. These suggest a relatively poor fit, implying that the model struggles to capture the full variability in Bitcoin’s price impact during these test periods. The observed discrepancies between train and test R^2 scores, especially where the test R^2 turns negative, indicate potential overfitting. A negative R^2 means the model’s predictive power is worse than a simple mean prediction. These negative test R^2 scores coincide with sharp spikes in λ_t values, hinting at instances where the model fails to generalize across different market conditions.

This volatility in λ_t suggests that illiquidity conditions in the Bitcoin market can shift rapidly within short time windows. This observation contrasts with the smoother λ_t estimates typically found in traditional financial markets [33]. The sharp intraday changes in λ_t highlight Bitcoin’s unique global and 24/7 market structure, where illiquidity and market impact can vary significantly depending on the overlap of international markets. While [19, 46] found that Bitcoin’s volatility and liquidity follow a predictable intraday cycle, the erratic behavior of λ_t suggests that Bitcoin’s market dynamics are still highly unpredictable, particularly during less liquid trading hours.

4.2.2 Variations in λ Throughout our Dataset

The observed discrepancy between the training and testing R^2 values, as illustrated in Figure 3, suggests that λ_t exhibits both intraday variability and potential changes across the dataset. These changes are not limited to fluctuations within a single trading day but may also shift over the months of the data analysed.

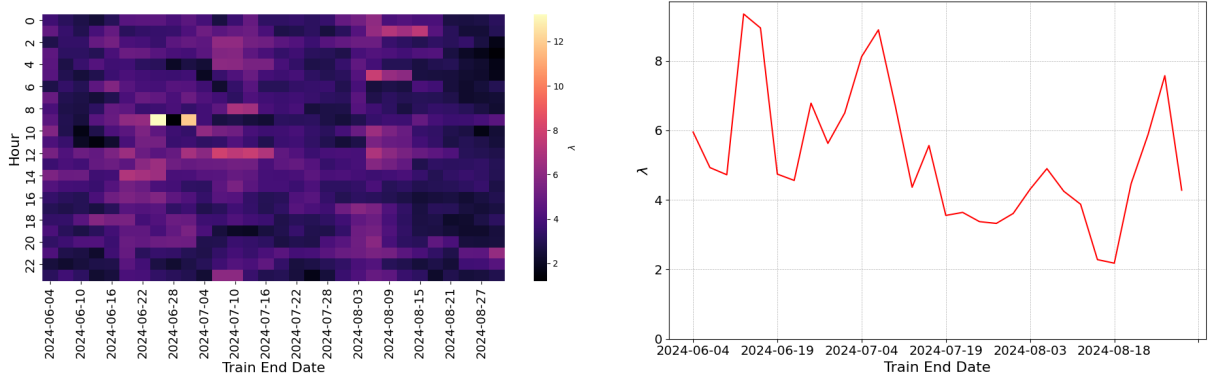


Figure 4: Heatmap showing the λ_t values across different end-of-training periods (left) and plot of the mean daily λ_t over the entire dataset (right). Both plots use the exponent $\delta = 0.35$ and identical training-testing periods.

The heatmap in Figure 4 reveals that λ_t fluctuates throughout the day, with lower values clustering during later hours. These periods of lower λ_t coincide with increased liquidity and reduced market impact, particularly after the opening of the European and US markets. This pattern reflects the strong influence of global trading hours on Bitcoin liquidity.

Moreover, the dataset demonstrates a general downward trend in daily λ_t values during August, as shown in Figure 4 (right), suggesting seasonal or periodic patterns in market impact. This broader temporal variability implies that λ_t not only fluctuates intraday but also evolves over longer horizons.

Volatility in λ_t , especially during active US trading hours, is accompanied by lower R^2 scores, as illustrated in Figure 3. These observations suggest that liquidity fluctuations and market noise may reduce model reliability during these periods, underscoring the importance of frequent retraining to account for dynamic market conditions.

Incorporating time-dependent variations in λ_t into the model is essential for achieving more accurate volume scheduling and market impact predictions. By retraining the model frequently, traders can avoid poor timing – such as trading too heavily during low-liquidity periods or missing opportunities in high-liquidity periods – thus minimising transaction costs and optimising execution strategies.

Given the variability in λ_t , extending both training and testing periods may yield more stable estimates and deeper insights into evolving market regimes. A longer dataset could also improve the robustness of predictive models, helping navigate liquidity shifts and changes in market conditions over time.

4.2.3 Optimising for δ

The exponent δ in the impact function determines how trading volume translates into impact state. Smaller values of δ mean that even relatively small trade volumes can have a noticeable effect on the market, while larger volumes only marginally increase the impact. This may indicate a market structure where the visible liquidity at the best bid or ask is shallow, but substantial liquidity exists deeper in the order book. In such cases, the initial market orders might not penetrate far enough to impact deeper levels, thus limiting the overall price movement despite large volumes traded.

Conversely, larger values of δ imply that price impact scales more sharply with volume. This reflects a market where liquidity is more evenly distributed across the order book. In this scenario, the difference between small and large volumes is more pronounced, indicating that the market can absorb volumes more uniformly without causing significant price changes, thereby making it harder for trades to avoid triggering substantial impacts.

After cross-validation, we aim to determine whether a particular value of δ consistently outperforms others or if the optimal δ varies depending on market conditions. Following the methodology of Coxon [16, Section 4.2], we plot the in-sample R^2 values for various cross-validation windows and across the full range of δ values, as shown in Figure 5. This analysis uses the same 7-day training and 3-day testing periods.

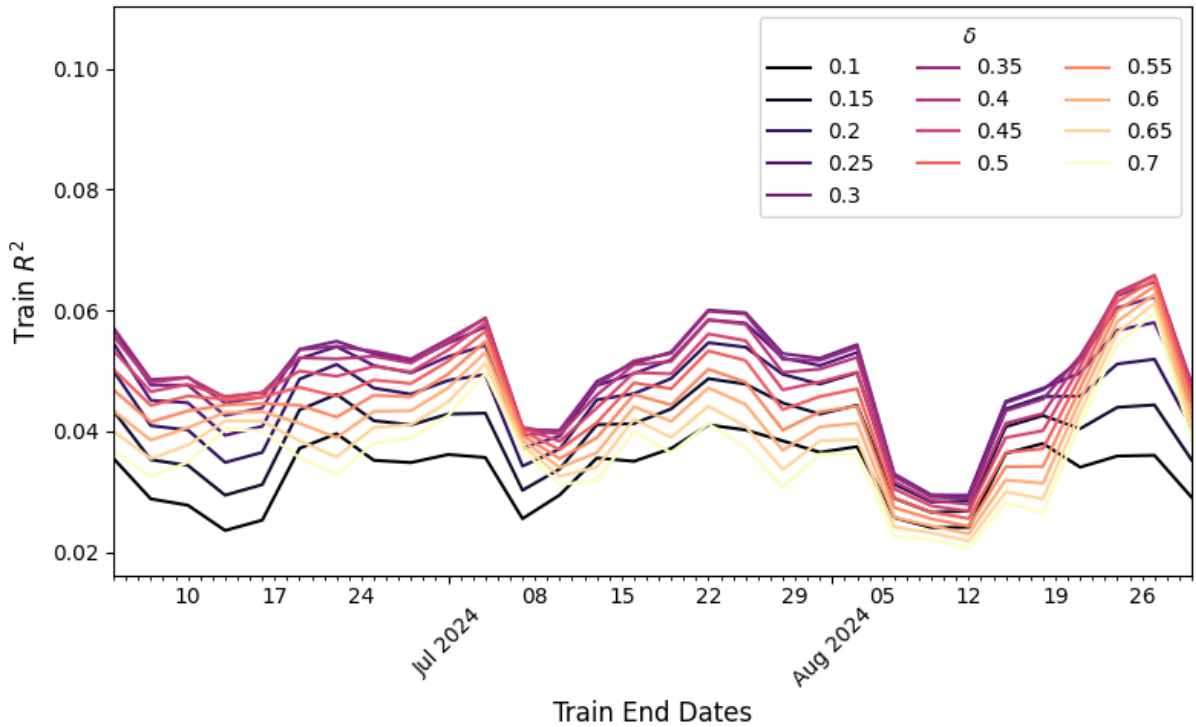


Figure 5: Train R^2 for different values of δ over time.

The plot shows that the train R^2 values remain consistently low throughout the

sample period, with only subtle differences in performance between the values of δ . Exponents in the mid-range, specifically $\delta \in [0.35, 0.50]$, appear to perform marginally better than those at the extremes, $\delta = 0.10$ and $\delta = 0.70$, though the differences are not substantial.

The relative flatness of the R^2 curves suggests that the model does not capture substantial temporal variations in market conditions. This stability may indicate that the DPM is insufficient in explaining the evolving dynamics of market impact, particularly over time. The consistently low R^2 values highlight potential limitations in the model’s ability to describe the relationship between impact returns and price returns.

One possible explanation for these results lies in the unique structure of Bitcoin’s market compared to traditional financial markets. Bitcoin’s public trading data may differ significantly from that of stock or futures markets, which typically have higher liquidity and different volatility characteristics. Additionally, the constant decay parameter β used in the model might not adequately reflect how price impact dissipates over time in cryptocurrency markets. A more flexible decay rate, such as a power-law decay form, could potentially yield more realistic impact dynamics across time bins, especially in markets where liquidity and trading activity vary throughout the day. The power-law decay form allows for slower fading of past trades’ influence, which may be more appropriate for markets like Bitcoin where liquidity distribution can be uneven across time.

Moreover, the fragmented nature of Bitcoin markets – spread across multiple exchanges with varying liquidity – makes it difficult for any single propagator model to accurately capture overall market impact. This fragmentation could contribute to the model’s inability to adequately explain price impact across time periods, especially when compared to more uniform markets.

In their study, Coxon [16] explored the impact of different training and testing window combinations on model performance, assessing the stability between in-sample (train) and out-of-sample (test) results. By examining metrics like the test-train ratio and maximum test regret, they were able to evaluate whether alternative parametrisations could have provided better fits during backtesting, particularly over extended periods of time. Their approach provided insights into how variations in model parameters such as λ and δ influenced the results across different time horizons.

However, this methodology is not pursued, primarily due to the constraints of the dataset. With only four months of data available – approximately three months, considering the 1-month lookback period required for calculating the SMAs described in Section 3.3 – we did not expect that experimenting with different train-test splits would significantly affect the R^2 scores. The data did not exhibit sufficient variability to justify a detailed investigation into alternative parametrisations. With access to a

larger dataset spanning multiple years, different combinations of training and testing windows could have been explored to capture potential changes in market dynamics and improve model robustness. Given the available data, the analysis prioritised simplicity and consistency with a fixed approach.

5 Optimal Trade Scheduling

The aim is to determine the optimal strategy for executing a large buy order of volume X within $[0, T]$. Although the literature review in Section 2 and other sections usually referred to the idea of finding an 'optimal trading strategy', the expression 'optimal trading schedule' is preferred from now on. The focus is on optimally scheduling the execution volume over time. These terms are interchangeable, and the theoretical frameworks discussed in relation to 'strategies' can be applied directly to the context of trade scheduling. Optimal trading schedules are derived for two scenarios: constant intraday illiquidity and time-dependent intraday illiquidity. The purpose will be to measure using different benchmarks whether performing an intraday analysis yields better results than a static estimation of illiquidity.

The assumption is that the price impact follows the dynamics outlined in Equation (2.17). Additionally, the effect of δ on the optimal trading schedule is explored. Introducing non-linear price impact complicates the optimisation process and can lead to price manipulation, an issue that remains poorly understood in non-linear models. Both the linear and non-linear cases are examined, investigating their relationship to price manipulation and the corresponding solutions to the optimal trading scheduling problem. The presence of any predictive trading signals is excluded in order to derive deterministic optimal trading schedules, following the approach of Obizhaeva and Wang [42].

5.1 Excess Cost Minimisation

Using the framework defined in Equation (2.8), the goal is to minimise the excess costs incurred by executing trades over time. The excess cost refers to the additional cost caused by the price impact of the trader's actions beyond the baseline market price. The price impact, represented by the state variable I_n , reflects the cumulative effect of all prior trades and is known at the start of time bin n . Using the principle defined in Equation (2.8), we define the total excess cost incurred over the trading period as the following cost function,

$$C = \sum_{n=1}^N I_n^m \cdot \Delta F_n^m. \quad (5.1)$$

Equation (5.1) calculates the additional cost incurred in each time bin n due to the market impact, summing the excess cost across all time bins from 1 to N . If the impact state I_n is high, indicating significant prior market impact, the trader incurs a higher excess cost for the volume traded in that bin. Conversely, if the market impact at time n is minimal ($I_n = 0$), no excess cost is incurred in that bin ($C_n = 0$).

The optimisation problem is to determine the sequence of trades $\{\Delta F_n\}$ that minimises the total excess cost

$$\min_{\{\Delta F_n^m\}} \sum_{n=1}^N I_n^m \cdot \Delta F_n^m \quad \text{s.t.} \quad \sum_{n=1}^N \Delta F_n^m = X_0, \quad (5.2)$$

The constraint ensures that the total volume traded over the time horizon equals X . I_n evolves according to the impact state dynamics in the DPM,

$$\Delta I_n^m = -\beta \Delta t I_{n-1}^m + \sigma_{\text{ret}}(m, 30) f\left(\frac{\Delta F_n^m}{V_{\text{avg}}(m, 30)}\right). \quad (5.3)$$

The realised excess costs due to market impact are minimised by optimal $\{\Delta F_n\}$. Unlike expected cost minimisation, which takes into account stochastic elements, this approach assumes deterministic market conditions and focuses purely on reducing the additional costs caused by the impact of executing trades.

5.2 Fixed Intraday Illiquidity

λ remains fixed throughout the trading day, resulting in a fixed illiquidity parameter $\bar{\lambda}$ over the time period $[0, T]$. This $\bar{\lambda}$ is derived by taking the mean value of λ_t values for that day. We fix every λ_t to this mean value. $\bar{\lambda}$ provides a single estimate of the market's illiquidity, which is used to model the execution process throughout the entire day.

By substituting the updated form for $f(v) = \bar{\lambda} \text{sgn}(v) |v|^\delta$ inside Equation (5.3), the new form of the impact state dynamics evolution according to the DPM is

$$\Delta I_n^m = -\beta \Delta t I_{n-1}^m + \sigma_{\text{ret}}(m, 30) \bar{\lambda} \text{sgn}\left(\frac{\Delta F_n^m}{V_{\text{avg}}(m, 30)}\right) \left|\frac{\Delta F_n^m}{V_{\text{avg}}(m, 30)}\right|^\delta. \quad (5.4)$$

5.2.1 Linear Impact Case

First, we investigate the behaviour of the optimal schedule in the linear impact case. This problem has already been solved under different frameworks. Curato, Gatheral, and Lillo [18] derived an explicit formula for optimal trading speed by analysing a continuous TIM. They formulate the execution cost as a function of trading speed and the resulting price impact over time. By applying optimisation techniques, they derived conditions under which the trading speed minimises the cost of execution while satisfying the liquidity constraint. Their work emphasised the relationship between the speed of trading and the resulting market impact, providing a practical framework for optimising trading schedules. This differs from the optimal execution under the DPM, which operates in fixed time intervals and assumes a deterministic impact structure.

The DPM assumes a constant trading rate and specific impacts within a single time bin, while the continuous model allows for smoother adjustments of trading speed in response to real-time market conditions.

When $\delta = 1$, the impact function simplifies to a linear relationship, making the impact state directly proportional to the traded volume. In this case, the impact state I_n^m becomes equal to the volume ΔF_n^m traded within a time bin, leading to the expression

$$I_n^m \cdot \Delta F_n^m = (\Delta F_n^m)^2. \quad (5.5)$$

For simplicity, the illiquidity and the normalisation of impact are disregarded in this explanation. Summing the impact costs across multiple time bins results in the following objective function, which takes the form of a sum of squared terms,

$$C = \sum_{n=1}^N (\Delta F_n^m)^2, \quad (5.6)$$

highlighting its quadratic nature. This transforms the minimisation problem into

$$\min_{\{\Delta F_n^m\}} \sum_{n=1}^N (\Delta F_n^m)^2 \quad \text{s.t.} \quad \sum_{n=1}^N \Delta F_n^m = X_0, \quad (5.7)$$

In sequential quadratic programming (SQP) optimisation, the optimisation problem is addressed by solving a series of quadratic programming sub-problems based on the quadratic approximation of the Lagrangian, which includes both the objective function and the constraint in Equation (5.2). In our implementation, we use the Sequential Least Squares Programming (SLSQP) algorithm from the Python package SciPy [44]. The SLSQP algorithm converges to a local minimum by satisfying the Karush-Kuhn-Tucker conditions. SLSQP can guarantee convergence to the global minimum, if the problem is well-defined and the objective function is convex. We do not go further into the theory of the algorithm.

As in Curato, Gatheral, and Lillo [18], we consider X to be a metaorder execution where a trader buys $X\%$ of the available unitary market volume. The interval $[0, T]$ is split into 15-minute time bins, giving us a total of 96 time bins for 24 hours of trading. We set $\delta = 1$ and consider a fixed market impact coefficient value $\bar{\lambda} = 1$ for all time bins. For the simple linear case, we assume a fixed $\sigma = 1$ to normalise the impact function. Additionally, we assume there is zero bid-ask spread in the market, implying that transactions can occur at the mid-price. This simplifies the model by excluding spread-related frictions, allowing us to focus purely on price impact.

The underlying methodology for optimising trading schedules is derived from open source code by [17]. A class that simulates trade scheduling based on discrete

price impact models is used throughout this section. The optimal trading volume in each period is shown in Figure 6.

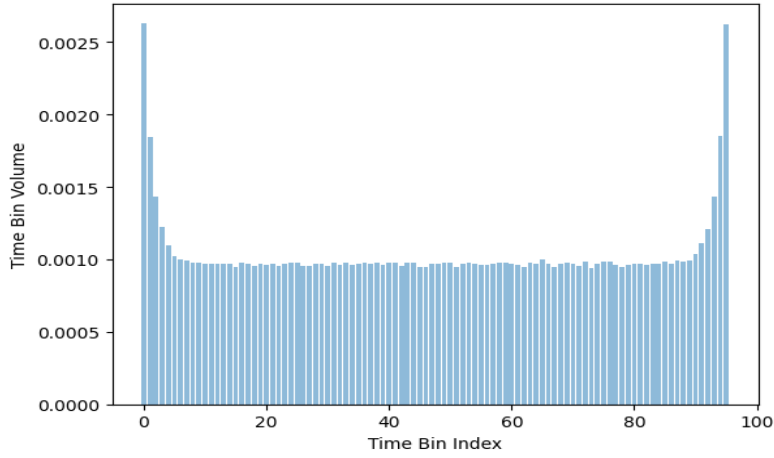


Figure 6: The optimal execution strategy calculated using the SLSQP method for $X_0 = 0.1$. The time horizon T is divided into 96 distinct time bins, corresponding to 4 trading intervals per hour over a 24-hour period. The y-axis represents the consistent average trading rate within each sub-interval. The minimum estimated expected execution cost is 5.59×10^{-4} .

The optimal strategy in the linear impact case appears to have good regularity. The solution has a perfectly symmetric output around the middle point of the day. The trading velocity (volume traded per time interval) is high at the beginning and equally high at the end of the trading day, with a constant speed in the middle. In addition, the strategy is consecutive, meaning that the trader is required to trade in all of time bins to fully minimise the execution cost. In addition, the buy program for the DPM with linear transient impact does not include selling. Such a strategy is a monotone one.

5.2.2 Non-linear Impact Case

In this section, the non-linear transient impact function is studied alongside the corresponding optimal trading schedule. The exponent δ is varied, ranging from slightly concave to strongly concave cases, to examine how the optimal strategy changes. Similar to the linear case, $\sigma = 1$ and no bid-ask spread are assumed. The numerical results for $\delta = \{0.95, 0.70, 0.50\}$ within f are presented in Figure 7.

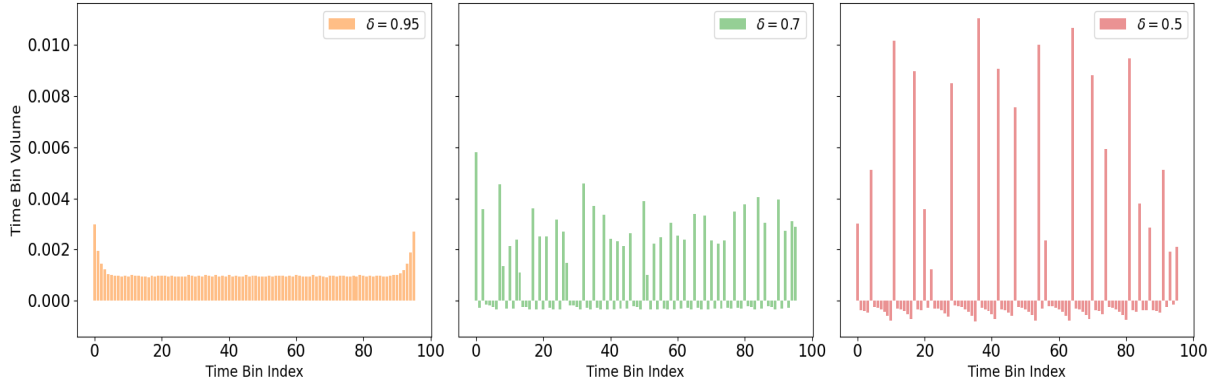


Figure 7: The optimal execution strategy determined using the SLSQP method for $X = 0.1$. The time horizon T is discretised into 96 time bins, with 4 trading intervals per hour over a full 24-hour period. The y-axis represents the average volume traded per time bin, illustrating the optimal rate of execution under different non-linearity exponents.

For the case where $\delta = 0.95$, the optimal strategy remains similar to the linear case. However, it executes trades slightly faster at the start of the day compared to the linear case (see Figure 6), with similar speed in the middle. While trading is fast at the end of the day, it is slower than at the start, resulting in a slightly asymmetric pattern, unlike the linear impact case.

For more concave cases, such as $\delta = 0.7$, the optimal trading schedule undergoes significant changes and is no longer monotone or single-signed [47]. Even in a buy program, there are intervals where the trader sells. After a series of small sells, the strategy switches to larger buy orders. The more consecutive sell orders occur, the higher the subsequent buy speed in the next bin. This represents a strategy designed to lower execution costs by selling small amounts before placing larger buy orders. However, this behavior aligns with the phenomenon of transaction-triggered price manipulation, where sell orders are introduced within a buy program [47, 18, 16]. Such strategies are forbidden.

In the strongly concave case, where $\delta = 0.5$, the optimal strategy becomes even more irregular. All periods of buying are interrupted by consecutive bursts of selling.

For $\delta = \{0.70, 0.50\}$, the expected execution costs of 3.5×10^{-3} and 7.0×10^{-3} , respectively, remain positive, despite the irregularity. These strategies do not lead to arbitrage opportunities.

5.2.3 Optimal Trading Schedule Across (δ, λ) Combinations

We move away from holding $\lambda = 1$ fixed. Instead, the λ values are now derived empirically, as detailed in Section 4.2.1. Specifically, $\bar{\lambda}$ is calculated as the average of the hourly market impact coefficients across the trading day of July 25, 2024, for each corresponding δ . We also include a fixed $\sigma = 2 \times 10^{-4}$, which aligns with the daily

averages calculated in Section 3.3. These values are assumed to hold over the longer 15-minute time bins, as the standard deviations σ are inherently related to the empirically determined λ values from the linear regressions performed in Section 4.1. The assumption of no bid-ask spread is maintained. Figure 8 presents the optimal strategies for $\delta \in \{0.7, 0.5, 0.3, 0.1\}$.

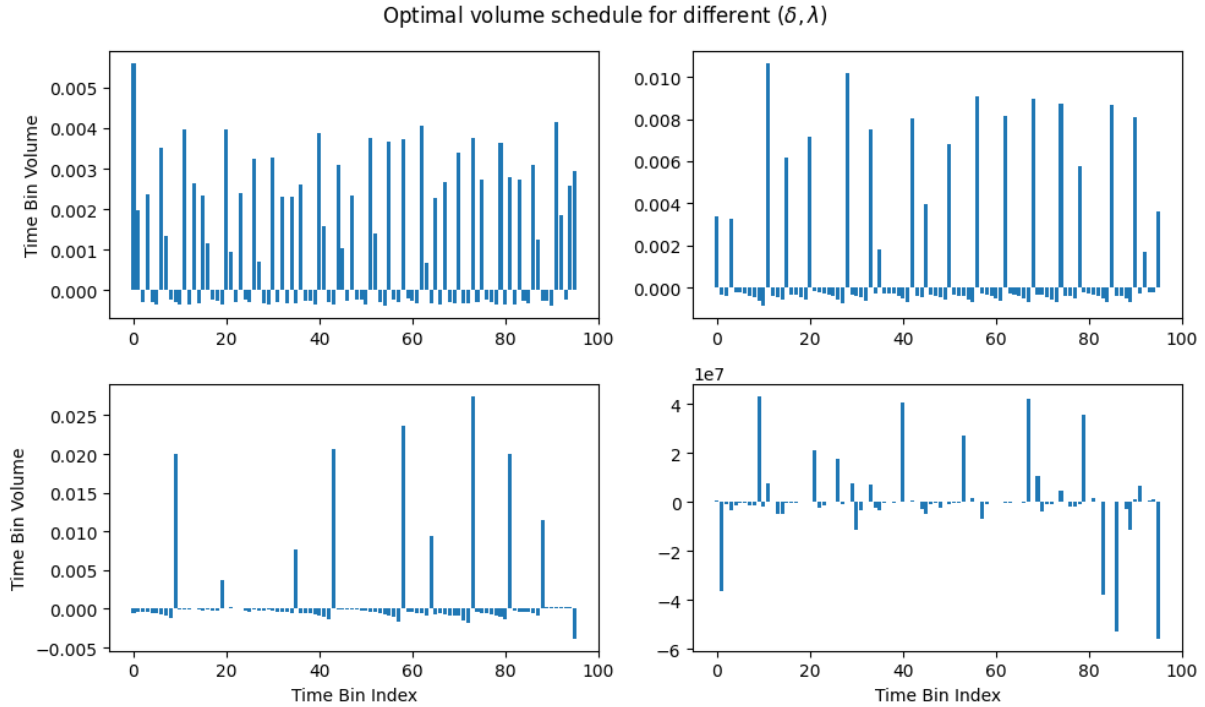


Figure 8: Optimal trading schedule for different combinations of δ and $\bar{\lambda}$. Each subplot illustrates the optimal volume distribution over 15-minute intervals during a trading day. The top left subplot corresponds to $(\delta, \bar{\lambda}) = (0.7, 40.54)$, the top right to $(0.5, 15.05)$, the bottom left to $(0.3, 3.99)$, and the bottom right to $(0.1, 0.52)$.

For $\delta = 0.3$, as discussed in Section 5.2.2, the strategy exhibits bursts of large buys followed by bursts of selling. The execution cost is slightly negative at -3×10^{-6} , hinting at inefficiencies in the strategy. When $\delta = 0.1$, the optimal strategy lacks discernible structure, with buy and sell orders exceeding the desired volume of $X = 0.1$ by an order of magnitude. The execution cost here is highly negative, at $-92,518$ units, indicating a price manipulation opportunity, as explored in Section 2.2. This suggests the potential for a round-trip strategy, generating positive revenue in expectation, thus implying arbitrage.

In contrast, for $\delta = 0.7$ and $\delta = 0.5$, the strategies yield positive expected execution costs of 2.9×10^{-5} and 2.1×10^{-5} , respectively, suggesting these cases are less prone to arbitrage. However, there are still sell orders in the buy program, with more frequent small buy orders compared to the more concave cases, reflecting a less aggressive execution strategy and the presence of transaction-triggered price manipulation.

We conclude that none of these strategies are viable for real-world applications. These results highlight both the limitations of the DPM and the drawbacks of using the SLSQP algorithm to solve for the optimal strategy. We conclude that the strategies found through the minimisation problem in the non-linear DPM in Equation (5.4), with $\delta < 1$, are not well-defined, as they allow for arbitrage opportunities.

5.2.4 Optimal Trading Schedule Across Trading Frequencies

Figure 9 shows the effect of changing the trading frequency on the optimal trading schedule.

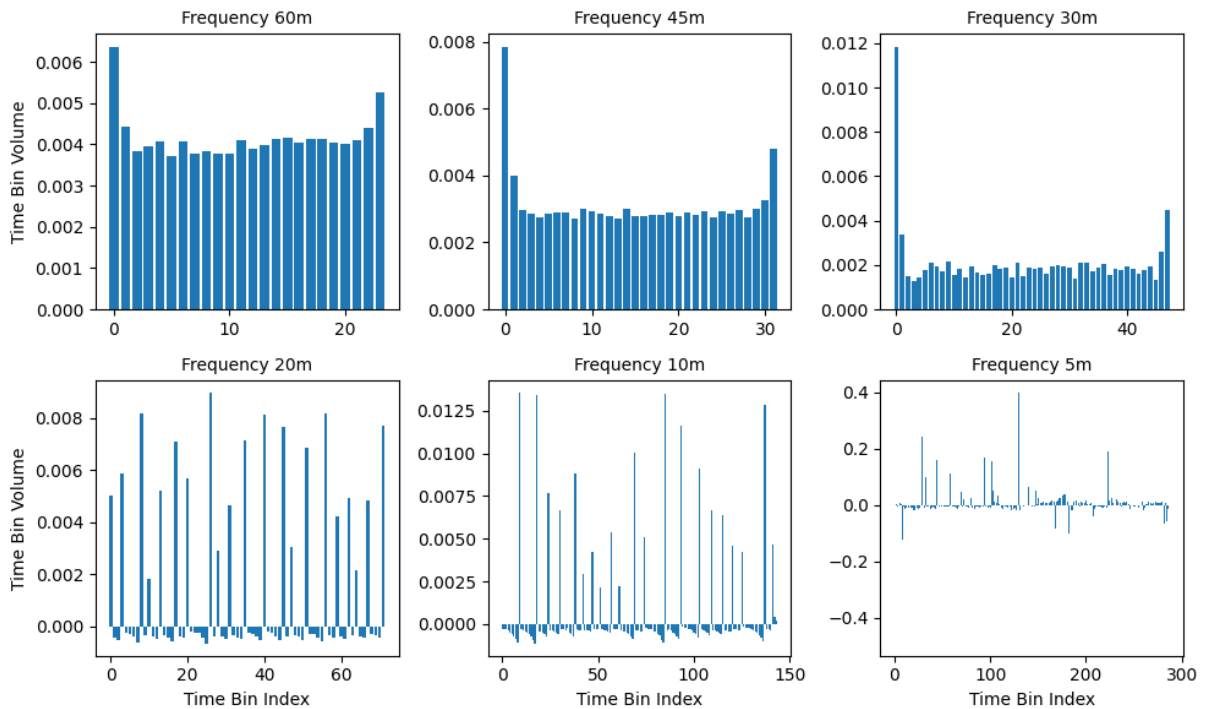


Figure 9: Optimal trading schedule for different time bin frequencies: 60, 45, 30, 20, 10, and 5 minutes. The propagator model parameters are set to $\delta = 0.5$, $\lambda \approx 15.05$, and a half-life of 1 hour.

For trading frequencies between 30 and 60 minutes, the strategies exhibit single-signed buy programs, while frequencies between 5 and 20 minutes introduce selling within the buy programs, consistent with earlier observations in this section. Lower trading frequencies produce smaller absolute volumes of trades compared to higher frequencies, but the 5-minute frequency program misbehaves, with both buy and sell trades occasionally exceeding the target volume of $X = 0.1$.

As trading frequency increases, the expected execution cost rises from 2.7×10^{-5} at the 60-minute frequency to 3.7×10^{-5} for the 30-minute frequency, coinciding with faster trading during the first hour of the trading day. For example, the 30-minute

frequency executes approximately 0.0125 units in the first hour, compared to 6×10^{-3} units at the 60-minute frequency. This higher trading speed likely explains the increased execution cost. As seen previously in Figures 6 and 7, both frequencies exhibit faster trading at the beginning and end of the day.

When selling appears in the buy program, and the solution becomes ill-defined, the expected execution cost decreases, dropping from 2.5×10^{-5} at the 20-minute frequency to a negative value of -6.6×10^{-4} for the 5-minute frequency. This suggests that higher trading frequencies may enable more effective exploitation of transaction-triggered price manipulation.

To verify the relationship between higher trading frequencies and increased manipulation potential, we plot the expected execution cost as a function of the degree of non-linearity δ , as shown by Wang [47] for various discretisations. The 5-minute frequency is excluded since the solution is ill-defined, and the SLSQP algorithm struggles to find an optimal solution across the entire range of δ considered in Figure 10.

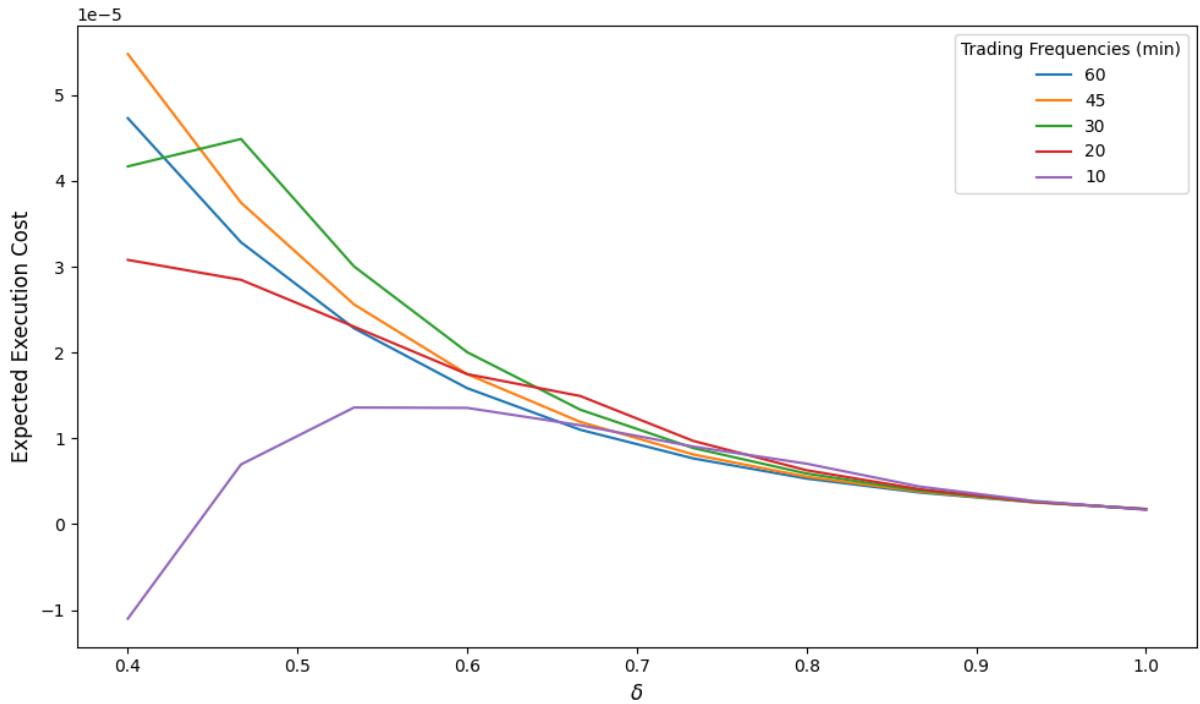


Figure 10: Optimal execution costs as a function of the degree of non-linearity, δ , across different trading frequencies. The range $\delta \in \{0.4, 0.5, \dots, 1.0\}$ is used. The impact coefficient $\bar{\lambda}$ is fixed, corresponding to $\delta = 0.5$.

Wang [47, Section 5.3] found that finer discretisations never lead to higher execution costs compared to coarser ones, regardless of the non-linearity degree δ . While that study used a continuous-time model discretised for practical computations with a power-law decay kernel, our model employs a discrete time recursive approach with an exponential decay kernel. Despite these differences, both approaches model transient

non-linear impact, and the optimal strategies obtained through SLSQP optimisation are comparable.

For $\delta \in [0.4, 0.8)$, there is no clear order of expected execution costs based on trading frequency. At low degrees of non-linearity, the discrepancy between execution costs across frequencies is more pronounced. The benefit of higher trading frequencies becomes more evident for strongly non-linear impact functions, as indicated by the negative execution cost at $\delta = 0.4$ for the 10-minute frequency. Smaller values of δ might yield even more negative costs if tested. However, for $\delta \in [0.8, 1.0)$, the results agree with Wang [47], where higher trading frequencies yielded higher execution costs. All cost lines converge at $\delta = 1$, where the linear impact model shows no dependence on trading frequency. It remains unclear whether this result stems from the properties of SLSQP optimisation or the transient nature of price impact.

5.2.5 Optimal Trading Schedule Across Bid-Ask Spreads

In all previous subsections, we assumed no bid-ask spread, meaning it was possible to buy and sell at the same mid-price. In reality, the bid-ask spread introduces an additional trading cost, similar to price impact. In the presence of a spread, a single trade costs the trader half the size of the spread, preventing round-trip trades from occurring at zero cost. According to the linear TIM in, the optimal strategy to execute an order depends on the dynamic properties of supply and demand, such as the recovery speed after a trade, rather than static properties like the bid-ask spread or market depth [42]. For the non-linear TIM, we account for the change in mid-price during execution, adding half of the bid-ask spread as an additional cost to our objective function in Equation (5.1), similarly to Equation (5.2),

$$\min_{\{\Delta F_n^m\}} \sum_{n=1}^N \left(I_n^m \cdot \Delta F_n^m + \frac{s_n^m}{2} \cdot |\Delta F_n^m| \right) \quad \text{s.t.} \quad \sum_{n=1}^N \Delta F_n^m = X_0, \quad (5.8)$$

where s_n^m is the bid-ask spread at the start of time bin n , at time t_{n-1} , on day m .

In the transient model, the bid-ask spread can be seen as a penalty against wrong-way trading [47]. This could help reduce or eliminate sell orders in a buy program, thus preventing transaction-triggered price manipulation. As Brodie et al. [12] noted, adding a penalty proportional to the sum of the absolute portfolio weights (i.e., L_1 -regularisation) stabilises the solution and excludes short positions. Similarly, the bid-ask spread imposes a cost that discourages non-monotonic strategies. Figure 11 shows the effect of increasing bid-ask spread values on the optimal trading schedule.

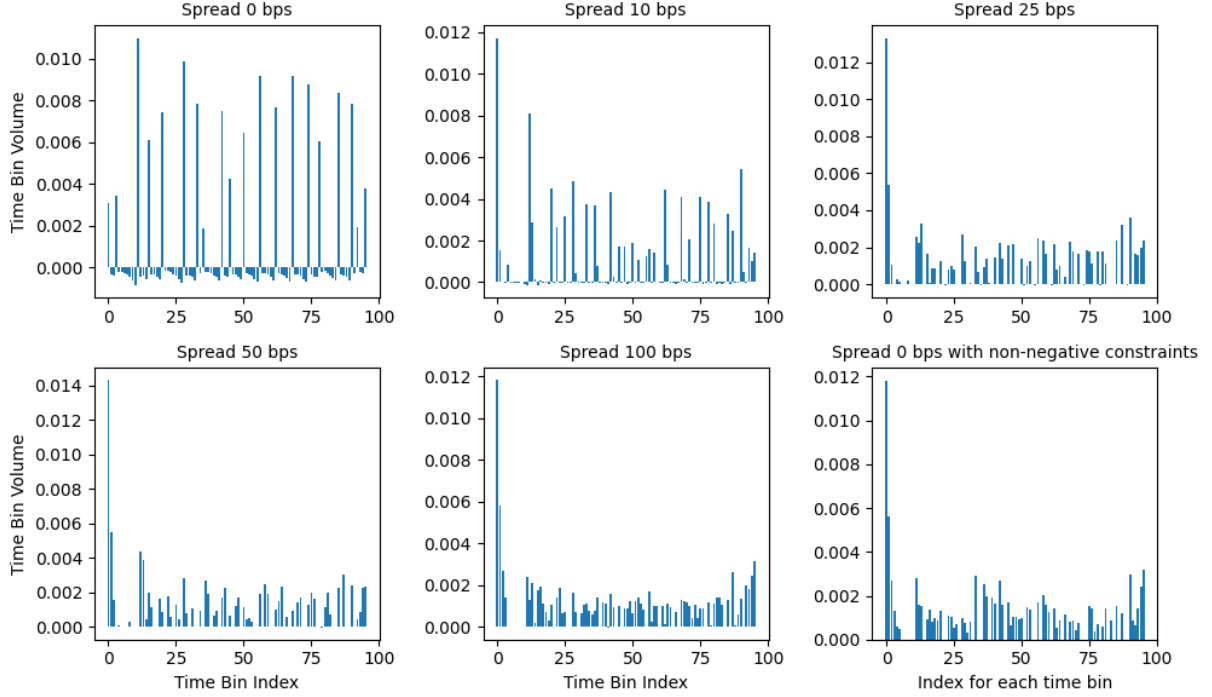


Figure 11: Optimal trading schedules under different bid-ask spread costs (0, 10, 25, 50, and 100 basis points) for $(\delta, \bar{\lambda}) = (0.5, 15.05)$. The subplots illustrate how increasing spread costs affect the distribution of trading volumes across time bins. The expected execution cost is shown for each case, and the final subplot displays only non-negative volumes traded within each time bin.

Without a bid-ask spread, the buy program includes short bursts of selling. Adding a 10 bps spread increases the expected execution cost from 2.1×10^{-5} to 3.2×10^{-5} and reduces the selling activity. Spreads of 25 and 50 bps further reduce sell orders, while a 100 bps spread nearly eliminates them. Table 3 lists the total negative volume (i.e., sells) for each spread level. In the final subplot, we enforce a monotone trading schedule by imposing a constraint that requires non-negative trading volume in each bin, i.e., $v_i \geq 0, \forall i$, similar to the no-short-selling constraint in portfolio optimisation [12].

Spread (bps)	Negative Volume
0	-3.16×10^{-2}
10	-2.31×10^{-3}
25	-5.28×10^{-4}
50	-1.75×10^{-4}
100	-4.47×10^{-5}

Table 3: These values reflect the total negative volume observed in the optimal trading schedules.

While larger spreads significantly reduce selling, they do not fully eliminate it. However, the spreads used here (up to 100 bps) are relatively high, particularly for a liquid cryptocurrency like Bitcoin on Kraken. To gauge a more realistic bid-ask spread,

we compute the mean spread from our dataset, which is 19 bps. Figure 12 shows the daily mean bid-ask spread over our dataset time frame. It shows that the mean bid-ask spread is skewed by large increases in spreads during periods of volatility, such as in early August. During calmer periods, the mean spread hovers between 5 and 15 bps.

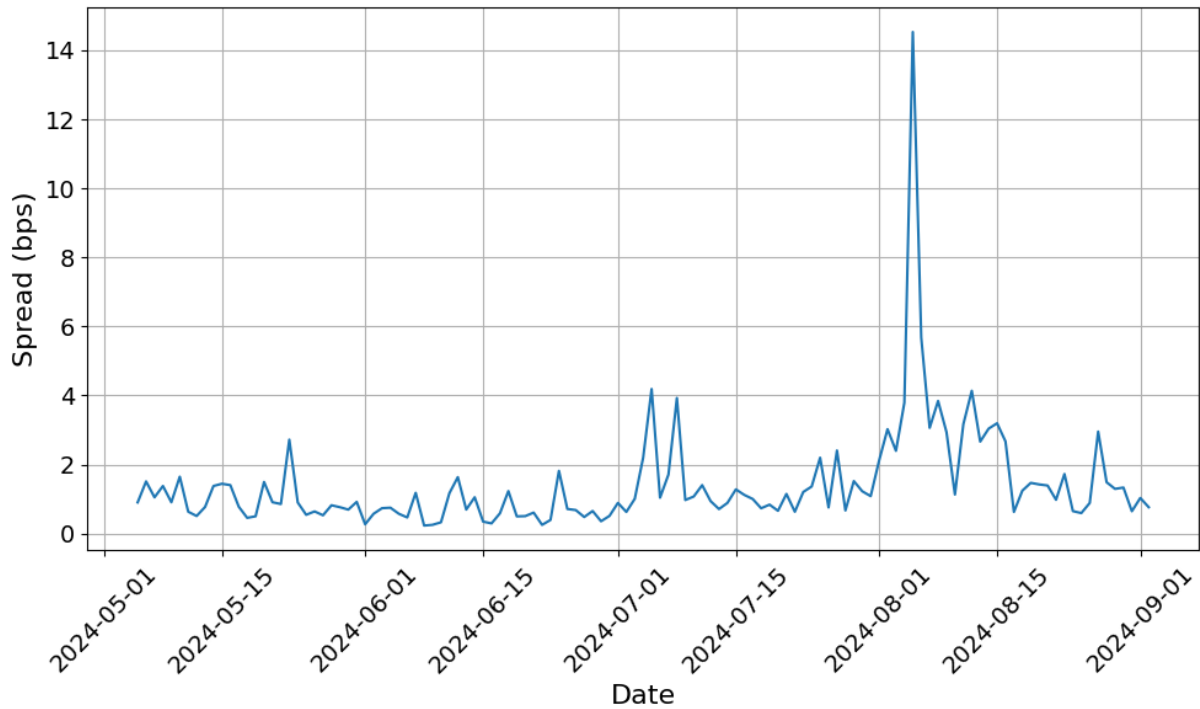


Figure 12: Daily mean bid-ask spread for the BTC/USD exchange rate over our dataset. The daily mean bid-ask spread is measured in basis points (bps), calculated as the difference between the best ask and bid quote prices normalised by the mid-price.

Assuming a constant bid-ask spread as large as 100 bps is unrealistic for a liquid market. These high spreads may be more appropriate for less liquid cryptocurrency pairs and exchanges. The only exception is during periods of high volatility or sharp declines. Market makers and liquidity providers minimise their risk by quoting wider spreads, while liquidity takers become more aggressive in executing trades, leading to illiquidity and price uncertainty. Additionally, assuming a constant bid-ask spread is an oversimplification, as the spread fluctuates with liquidity. Figure 12 illustrates the Modelling a time-varying spread would add complexity since it is closely tied to market conditions. For instance, after a large buy order clears the best ask, the spread could temporarily widen. However, this transient effect is not accounted for in our model.

5.3 Time-Dependent Intraday Illiquidity

In Section 4.2.1, we have found evidence that the intraday illiquidity shows time-of-day effects. It is thus of interest to include this information in our minimisation of excess costs process and find a corresponding optimal trading schedule.

By using the updated form for $f(v) = \lambda_t \text{sgn}(v)|v|^\delta$, the new form of the impact state dynamics evolution according to the DPM with time-dependent is

$$\Delta I_n^m = -\beta \Delta t I_{n-1}^m + \sigma_{\text{ret}}(m, 30) \lambda_t \text{sgn}\left(\frac{\Delta F_n^m}{V_{\text{avg}}(m, 30)}\right) \left| \frac{\Delta F_n^m}{V_{\text{avg}}(m, 30)} \right|^\delta. \quad (5.9)$$

The conclusions drawn from Section 5.2 are used to generate only transaction-triggered price manipulation-free strategies. These calculated excess costs are compared with well-know industry benchmarks and the excess costs generated by an optimal trading schedule assuming constant illiquidity.

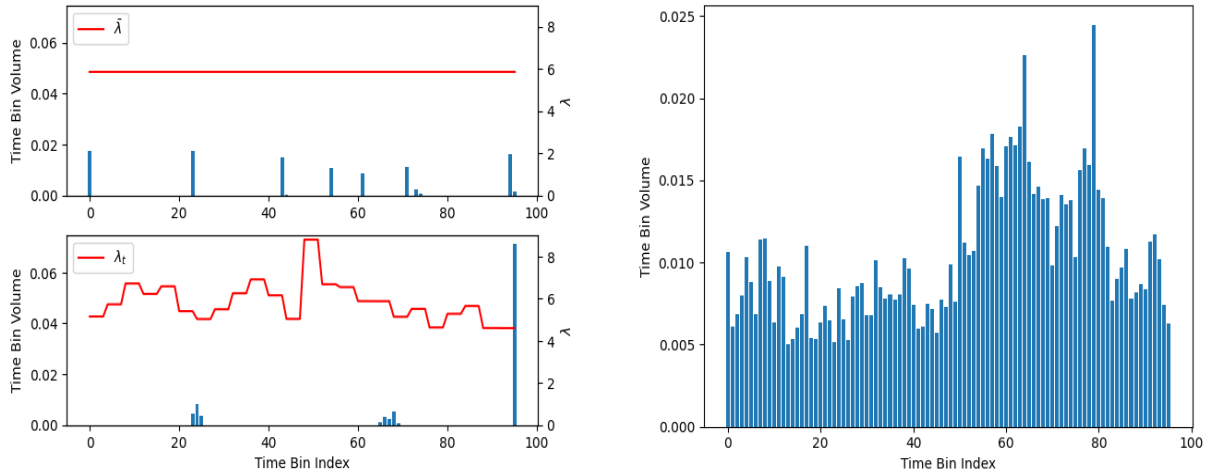


Figure 13: The optimal trading schedule for BTC/USD using historical volume data from July 1, 2024, comparing $\bar{\lambda} = 5.83$ (top left) and λ_t (bottom left). The bar plots show the volume traded in each time bin, while the red line depicts λ values. The strategy assumes $\delta = 0.35$ and $X = 0.1$, with a 15-minute time bin frequency. VWAP strategy for BTC/USD using historical volume data from July 25, 2024 (right). The volume traded in each bin is based on the VWAP calculation, with a 15-minute time bin frequency.

In the left plot of Figure 13, the trading volume in the top subplot for is sparsely distributed across time bins. The majority of trading activity occurs in select bins, with low and infrequent volumes. This indifference to hourly illiquidity could explain the sparsity of the volume. In contrast, the bottom subplot displays the time-dependent λ_t case, where the red line fluctuates throughout the day rather than remaining constant. This results in a different optimal trading schedule: volumes are concentrated in fewer time bins as the model adjusts dynamically to changes in λ_t . Periods of lower λ_t

are associated with higher trading volumes, while periods of higher λ_t lead to reduced activity. Notably, between index 30 and 70, a spike in λ_t leads to no traded volume, reflecting the model's tendency to align trades with periods of increased liquidity. The highest traded volume occurs in the final bin, where nearly 70% of the total volume is scheduled. This corresponds to the 15-minute interval with the lowest illiquidity. However, the concentration of such a large volume in a single bin may suggest that the model does not fully account for the price impact of its own trades within that bin, which might be addressed by more advanced techniques such as dynamic programming. This behaviour suggests that the simplifications made in the model could lead to unrealistic predictions and costs, especially as it does not consider factors like order book depth.

The right plot of Figure 13 shows the VWAP approach, which mimics the shape of the observed trading volumes across the day. Unlike the optimised schedules in the left plots, the VWAP schedule distributes trading activity more evenly across the day, with higher volumes in the middle of the trading session. This strategy closely follows market activity but does not account for illiquidity dynamics like the left plot.

This analysis follows that of Coxon [16, Section 5.3.1]. The focus is on comparing the execution costs associated with different trading schedules, using several industry benchmarks for evaluation. The following are examined.

- *Time-Weighted Average Price (TWAP)*: This strategy spreads the scheduled trading volume evenly across the trading period, ignoring changes in market conditions or liquidity.
- *Volume-Weighted Average Price (VWAP)*: This strategy executes trades proportional to the historical volume traded in each time bin. It aligns with trading patterns and is thus more adaptive than TWAP.
- *Market Open*: This strategy places the entire volume at the start of the trading day. It assumes that executing trades as early as possible avoids price drifts that could occur later in the day. It could lead to significant impact if the liquidity is low at market open.
- *Constant $\bar{\lambda}$ Strategy*: This strategy optimises a trading schedule under the assumption of constant illiquidity, represented by $\bar{\lambda}$, that is calibrated using empirical data.
- *Time-Dependent λ_t Strategy*: This strategy adjusts the trading schedule dynamically based on time-dependent illiquidity λ_t . It is calibrated hourly over the trading day.

Only the last two strategies incorporate any empirical calibration of illiquidity parameters. Only VWAP uses historical volumes to schedule trades. TWAP and Market Open do not incorporate any empirical data. In Table 4, the costs for various trading strategies are summarised.

X	δ	$\bar{\lambda}$	TWAP	VWAP	Market Open	Constant	Intraday
0.025	0.35	6.50	0.09	0.10	0.08	0.05	0.06
0.05	0.35	6.50	0.24	0.25	0.22	0.13	0.14
0.10	0.35	6.50	0.60	0.65	0.55	0.37	0.36
0.25	0.35	6.50	2.07	2.23	1.90	1.34	1.62

Table 4: Execution cost comparison across various trading strategies for total volumes $X \in \{0.025, 0.05, 0.1, 0.25\}$. All results are calculated with fixed value $\delta = 0.35$. Only the "Constant" strategy uses the fixed value $\bar{\lambda} = 6.50$.

First, it is clear that as X increases, so do the trading costs. Trivially, the more trading is scheduled, the more impact and thus excess costs are generated by the trading activity. Second, it appears as though the TWAP trading schedule outperforms the VWAP trading schedule. This may be due to the VWAP strategy trading during both high-volume and highly-illiquid periods in the trading day. It could then suggest that intraday periods showing high volumes do not necessarily correspond to periods where impact is minimum for executing large trades.

The "Market Open" strategy shows slightly lower costs than TWAP and VWAP strategies. The "Constant" and "Intraday" strategies, however, outperform all other strategies. For all volumes, the "Intraday" strategy exhibits higher costs than the "Constant" strategy. Taking into account λ_t does not necessarily offer a cost advantage.

For larger volumes, the "Constant" strategy consistently performs better than TWAP and VWAP, indicating that constant illiquidity models optimise trading schedules for larger volumes more effectively. The "Intraday" strategy, however, exhibits higher execution costs than the "Constant" strategy for these volumes. The spikes in λ (as seen in Figure 13) could be amplifying the cost of trades during these low-liquidity periods, despite the dynamic adjustments in trade scheduling.

The "Market Open" strategy performs competitively with the benchmarks at lower volumes but becomes less efficient at higher volumes, where the constant and intraday strategies take clear precedence. The increasing inefficiency of the "Market Open" strategy as volume grows suggests that concentrating trades within a short time period may not be optimal for larger orders, as it fails to account for liquidity dynamics across the entire trading day.

Overall, the findings suggest that while time-dependent illiquidity models can be beneficial in specific scenarios, particularly for small to medium volumes, a fixed $\bar{\lambda}$ approach remains competitive and even outperforms in minimising expected execution

costs. This calls into question the necessity of using more complex dynamic illiquidity models, particularly when simpler models such as the "Constant" strategy can provide cost-efficient solutions for significant trade volumes.

We also only use the single optimised pair for $(\delta, \bar{\lambda})$, so the performance of the trading schedules is not compared across values of δ .

Table 5 illustrates the relative cost savings of using the Intraday λ_t strategy as the baseline, compared to the other industry benchmarks. Negative savings indicate that the intraday strategy failed to yield a trading schedule with lower execution costs for the same volume and parameters.

For small trade volumes like $X = 0.025$, the baseline strategy saves significant percentages of the execution costs when compared the TWAP (40.44%), VWAP (44.8%), and Market Open (34.99%) strategies. However, the Constant $\bar{\lambda}$ strategy actually generates lower execution costs than the Intraday strategy, resulting in negative savings (-4.02%), implying that the Constant strategy outperforms the Intraday approach slightly for very small volumes.

When the volume reaches $X = 0.25$, the savings drop considerably across all strategies. The Intraday strategy provides only 21.95% savings compared to TWAP and 27.66% compared to VWAP. Interestingly, the Constant $\bar{\lambda}$ strategy exhibits the largest negative savings (-20.49%), indicating that it significantly outperforms the Intraday strategy at this higher volume.

X	δ	$\bar{\lambda}$	TWAP	VWAP	Market Open	Constant
0.025	0.35	6.5	40.44%	44.80%	34.99%	-4.02%
0.05	0.35	6.5	40.71%	45.04%	35.28%	-3.93%
0.1	0.35	6.5	40.68%	45.02%	35.25%	3.73%
0.25	0.35	6.5	21.95%	27.66%	14.80%	-20.49%

Table 5: Relative savings of using the Intraday λ_t strategy compared to industry benchmarks TWAP, VWAP, Market Open and Constant $\bar{\lambda}$ across different volumes X .

5.4 Summary

The section on optimal trading schedules presents a comprehensive comparison of various trading strategies, focusing on the effectiveness of time-dependent and constant illiquidity models. For smaller trade volumes, the time-dependent intraday λ_t strategy shows significant cost savings when compared to traditional industry benchmarks such as Time-Weighted Average Price (TWAP), Volume-Weighted Average Price (VWAP), and the Market Open strategy. These results indicate that dynamically adjusting the trading schedule to reflect intraday liquidity changes offers a substantial advantage for managing smaller orders. However, as the trade volume increases, the

relative savings from the intraday strategy diminish. The analysis also shows that the constant $\bar{\lambda}$ strategy outperforms the intraday λ_t model for larger orders especially.

6 Conclusion

6.1 Conclusion

This thesis has achieved two primary objectives: modelling price impact and optimising trading schedules in the context of cryptocurrency markets, specifically the BTC/USD pair. By addressing non-linear transient price impact, intraday liquidity fluctuations, and impact decay, we calibrated the DPM using public data.

We implemented a sliding-window cross-validation method to adapt to short-term market dynamics, recalibrating the model every three days. The DPM showed limited predictive power in explaining BTC/USD price changes through traded volume, with low and occasionally negative R^2 values. This raises questions regarding the model's generalisability to cryptocurrencies, as its performance contrasts with traditional asset markets.

The optimisation of trading schedules, based on calibrated δ and λ , aligned with the literature. Instances of transaction-triggered price manipulation required adjustments, like the inclusion of bid-ask spreads, reduced trading frequency, and constraints on negative volumes. These adjustments brought the model closer to realistic trading conditions.

Comparative analysis against industry benchmarks such as TWAP, VWAP, and Market Open demonstrated significant execution cost savings, averaging 35.39%. However, when compared to the constant $\bar{\lambda}$ strategy, the intraday liquidity model underperformed, resulting in a negative cost reduction of -6.18%. This indicates that, within our model, accounting for intraday liquidity did not consistently yield better outcomes.

This study provides valuable insights for institutions with limited proprietary data, offering a framework to reduce execution costs using public tape data. The findings highlight the importance of further refinement in modelling intraday liquidity for high-turnover environments, particularly within cryptocurrency markets.

6.2 Future Work

A key limitation of the DPM lies in its assumption that the price impact within each time bin is stationary. For instance, it assumes that executing a large volume of trades at the end of the day, when liquidity is highest, does not generate additional impact beyond what is already accounted for. However, in practice, trading itself dynamically affects liquidity within the bin. The assumption that the functional form of f remains unchanged at high trading rates may not hold. Literature suggests that market impact may become convex at elevated trading speeds, implying that the liquidity in the mar-

ket order book becomes insufficient to absorb rapid trades. Future research should consider modifying f to penalise high trading rates.

Another important direction would be to explore the low predictive power of the DPM, as indicated by low R^2 scores. It would be valuable to extend this analysis to other cryptocurrencies and exchanges to identify whether these shortcomings are specific to BTC/USD or represent a broader limitation of the model when applied to cryptocurrency markets. Considering the cross-impact between multiple assets is also necessary in future work. In real-world trading, the execution of trades in one asset can impact the prices of related assets.

Another area of interest involves the exploration of dynamic models that account for variations in limit order book depth, which is a crucial aspect of liquidity. The current model overlooks order book depth, focusing only on volume and illiquidity. Incorporating depth into the model could make the model more adaptable to different market conditions.

Another important area for future research lies in the relationship between bid-ask spreads and liquidity. Bid-ask spreads, which reflect market illiquidity, could be further examined within the context of the model, especially in terms of how spread fluctuations align with intraday liquidity changes. Future studies could investigate whether bid-ask spreads serve as more accurate real-time indicators of illiquidity, potentially improving trading schedule optimisation.

Lastly, future research should explore the distinction between price movements driven by trades and those caused by random market fluctuations. The inability to isolate these factors introduces noise into market impact models, complicating the interpretation of results. Further study could lead to more robust methods for distinguishing between trade-driven and random price movements, enhancing the accuracy of market impact predictions.

By addressing these limitations and exploring these directions, future research can build on the foundations laid in this thesis to improve the accuracy and utility of market impact models and optimised trading strategies.

References

- [1] Aurélien Alfonsi, Alexander Schied, and Alla Slynko. “Order book resilience, price manipulation, and the positive portfolio problem”. In: *SIAM Journal on Financial Mathematics* 3 (1 2012), pp. 511–533. doi: 10.1137/110822098.
- [2] F. Almgren et al. “Direct estimation of equity market impact”. In: *Risk* 18.7 (2005), pp. 58–62.
- [3] Robert Almgren. “Optimal execution with nonlinear impact functions and trading-enhanced risk”. In: *Risk* 10 (1 2003), pp. 1–18. doi: 10.1080/135048602100056.
- [4] Robert Almgren and Neil Chriss. “Optimal execution of portfolio transactions”. In: *Journal of Risk* 3.2 (2000), pp. 5–39. doi: 10.21314/JOR.2001.041.
- [5] Robert Almgren and Neil Chriss. “Value under liquidation”. In: *Risk* 12.12 (1999), pp. 61–63.
- [6] Louis Bachelier. “Théorie de la spéculation”. In: *Annales Scientifiques de l’École Normale Supérieure* 3.17 (1900). English translation by D. May (2011), pp. 21–86. URL: http://archive.numdam.org/article/ASENS_1900_3_17__21_0.pdf.
- [7] Dimitris Bertsimas and Andrew Lo. “Optimal control of execution costs”. In: *Journal of Financial Markets* 1.1 (1998), pp. 1–50. doi: 10.1137/S0363012995291609.
- [8] S. Bochner. *Vorlesungen über Fouriersche Integrale*. Leipzig: Akademische Verlagsgesellschaft, 1932.
- [9] J. P. Bouchaud et al. “Fluctuations and response in financial markets: The subtle nature of random price changes”. In: *Quantitative Finance* 4.2 (2004), pp. 176–190. doi: 10.1080/14697680400000022.
- [10] J.-P. Bouchaud, J. D. Farmer, and F. Lillo. “How markets slowly digest changes in supply and demand”. In: *Handbook of Financial Markets: Dynamics and Evolution*. Amsterdam, Netherlands: Elsevier, 2009, pp. 57–160. doi: 10.1016/B978-012374258-2.50004-7.
- [11] Jean-Philippe Bouchaud et al. *Trades, Quotes and Prices: Financial Markets Under the Microscope*. Cambridge, UK: Cambridge University Press, 2018.
- [12] Joshua Brodie et al. “Sparse and table markowitz portfolios”. In: *Proceedings of the National Academy of Sciences of the United States of America* 106 (Aug. 2009), pp. 12267–72. doi: 10.1073/pnas.0904287106.
- [13] Frederic Bucci. “Market impact for large institutional investors: empirical evidences and theoretical models”. Accessed on August 1, 2024. PhD thesis. Scuola Normale Superiore, 2020. URL: <http://hdl.handle.net/11384/90464>.

- [14] Enzo Busseti and Fabrizio Lillo. “Calibration of optimal execution of financial transactions in the presence of transient market impact”. In: *Journal of Statistical Mechanics: Theory and Experiment* 09 (2012). doi: 10.1088/1742-5468/2012/09/P09010.
- [15] R. Cont, A. Kukanov, and S. Stoikov. “The price impact of order book events”. In: *Journal of Financial Econometrics* 12.1 (2013), pp. 47–88. doi: 10.1093/jjfinec/nbt003.
- [16] G. Coxon. “Optimal Execution with Intraday Liquidity Changes and Transient Nonlinear Impact”. Accessed on August 1, 2024. MSc thesis. Department of Mathematics, Imperial College London, 2022. URL: <https://www.imperial.ac.uk/mathematics/postgraduate/msc/mathematical-finance/project-and-thesis/>.
- [17] George Coxon. *Price Impact Modelling*. Accessed: 2024-09-24. 2023. URL: https://github.com/georgec123/price_impact.
- [18] Gianbiagio Curato, Jim Gatheral, and Fabrizio Lillo. “Optimal execution with non-linear transient market impact”. In: *Quantitative Finance* 17.1 (Jan. 2017), pp. 41–54. doi: 10.1080/14697688.2016.1181274.
- [19] A. Eross et al. “The intraday dynamics of bitcoin”. In: *Research in International Business and Finance* 49 (2019), pp. 71–81. doi: 10.1016/j.ribaf.2019.01.008.
- [20] A. Frazzini, R. Israel, and T. J. Moskowitz. *Trading costs*. 2018. doi: 10.2139/ssrn.3229719.
- [21] Xavier Gabaix et al. “Institutional Investors and Stock Market Volatility”. In: *The Quarterly Journal of Economics* 121.2 (2006), pp. 461–504. doi: 10.1162/qjec.2006.121.2.461.
- [22] Jim Gatheral and Alexander Schied. “Dynamical Models of Market Impact and Algorithms for Order Execution”. In: *Handbook on Systemic Risk*. Ed. by Jean-Pierre Fouque and Joseph A. Langsam. Cambridge, UK: Cambridge University Press, 2013, pp. 579–599. doi: 10.2139/ssrn.2034178.
- [23] Jim Gatheral and Alexander Schied. “Optimal Trade Execution under Geometric Brownian Motion in the Almgren and Chriss Framework”. In: *International Journal of Theoretical and Applied Finance* 14.3 (2011). Available at SSRN: <https://ssrn.com/abstract=1654151>, pp. 353–368.
- [24] Olivier Guéant. *Permanent market impact can be nonlinear*. 2014. arXiv: 1305.0413 [q-fin.TR]. URL: <https://arxiv.org/abs/1305.0413>.
- [25] J. Hasbrouck. “Measuring the information content of stock trades”. In: *Journal of Finance* 46.1 (1991), pp. 179–207. doi: 10.1111/j.1540-6261.1991.tb03749.x.

- [26] Joel Hasbrouck and Duane J. Seppi. “Common factors in prices, order flows, and liquidity”. In: *Journal of Financial Economics* 59.3 (2001), pp. 383–411. DOI: 10.1016/S0304-405X(00)00091-X.
- [27] Natascha Hey et al. “The cost of misspecifying price impact”. In: *SSRN Electronic Journal* (2023). DOI: 10.2139/ssrn.4362817.
- [28] Robert W. Holthausen, Richard W. Leftwich, and David Mayers. “The effect of large block transactions on security prices: A cross-sectional analysis”. In: *Journal of Financial Economics* 19.2 (1987), pp. 237–267. DOI: 10.1016/0304-405X(87)90004-3.
- [29] Gur Huberman and Werner Stanzl. “Price Manipulation and Quasi-Arbitrage”. In: *Econometrica* 72.4 (2004), pp. 1247–1275. DOI: 10.1111/j.1468-0262.2004.00531.x.
- [30] Eduardo Abi Jaber and Eyal Neuman. *Optimal Liquidation with Signals: the General Propagator Case*. 2022. DOI: 10.2139/ssrn.4264823. arXiv: 2211.00447 [q-fin.TR].
- [31] Florian Klöck, Alexander Schied, and Yuemeng Sun. *Price manipulation in a market impact model with dark pool*. 2014. arXiv: 1205.4008 [q-fin.TR]. URL: <https://arxiv.org/abs/1205.4008>.
- [32] Petter N. Kolm, Jeremy Turiel, and Nicholas Westray. “Deep Order Flow Imbalance: Extracting Alpha at Multiple Horizons from the Limit Order Book”. In: *SSRN Electronic Journal* (2021). DOI: 10.2139/ssrn.3900141.
- [33] Albert S. Kyle. “Continuous Auctions and Insider Trading”. In: *Econometrica* 53.6 (1985), pp. 1315–1335. DOI: 10.2307/1913210.
- [34] Fabrizio Lillo, J Doyne Farmer, and Rosario N Mantegna. “Single curve collapse of the price impact function for the New York Stock Exchange”. In: *Nature* 421 (2002), pp. 129–130. DOI: 10.48550/arXiv.cond-mat/0207428.
- [35] F. Loeb. “Trading cost: The critical link between investment information and results”. In: *Financial Analysts Journal* 39.3 (1983), pp. 39–44. DOI: 10.2469/faj.v39.n3.39.
- [36] Christopher Lorenz and Alexander Schied. *Drift Dependence of Optimal Trade Execution Strategies Under Transient Price Impact*. Finance Stochastics, Forthcoming. 2013. DOI: 10.2139/ssrn.1993103.
- [37] Julian Lorenz and Robert Almgren. “Mean–Variance Optimal Adaptive Execution”. In: *Applied Mathematical Finance* 18.5 (2011), pp. 395–422. DOI: 10.1080/1350486X.2011.560707.

- [38] Jonathan R. Macey and Maureen O'Hara. "The Law and Economics of Best Execution". In: *Journal of Financial Intermediation* 6.3 (July 1997), pp. 188–223.
- [39] Johannes Muhle-Karbe, Zexin Wang, and Kevin Webster. "Stochastic Liquidity as a Proxy for Nonlinear Price Impact". In: *Operations Research* 72.2 (2023). DOI: 10.1287/opre.2022.0627.
- [40] S. Nakamoto. *Bitcoin: A Peer-to-Peer Electronic Cash System*. Retrieved from <https://bitcoin.org/bitcoin.pdf>. 2008.
- [41] Eyal Neuman and Moritz Voß. *Optimal Signal-Adaptive Trading with Temporary and Transient Price Impact*. 2022. DOI: 10.48550/arXiv.2002.09549. arXiv: 2002.09549 [q-fin.TR].
- [42] Anna A. Obizhaeva and Jiang Wang. "Optimal trading strategy and supply/demand dynamics". In: *Journal of Financial Markets* 16.1 (2013), pp. 1–32. ISSN: 1386-4181. DOI: 10.1016/j.finmar.2012.09.001. URL: <https://www.sciencedirect.com/science/article/pii/S1386418112000328>.
- [43] Torsten Schoeneborn and Alexander Schied. "Liquidation in the Face of Adversity: Stealth vs. Sunshine Trading". In: *EFA 2008 Athens Meetings Paper* (2009). DOI: 10.2139/ssrn.1007014.
- [44] SciPy Community. *SciPy API: Optimization and Root Finding (scipy.optimize)*. Accessed: 2024-09-05. 2024. URL: <https://docs.scipy.org/doc/scipy/reference/generated/scipy.optimize.minimize.html>.
- [45] Tardis.dev. *Tardis.dev Documentation*. <https://docs.tardis.dev/docs>. Accessed: 2024-08-01. 2024.
- [46] Jying-Nan Wang, Hung-Chun Liu, and Yuan-Teng Hsu. "Time-of-day periodicities of trading volume and volatility in Bitcoin exchange: Does the stock market matter?" In: *Finance Research Letters* 34 (2020), p. 101243. ISSN: 1544-6123. DOI: 10.1016/j.frl.2019.07.016.
- [47] Weiguan Wang. "Optimal Execution Under Nonlinear Transient Market Impact Model". Accessed on August 1, 2024. MSc thesis. University College London, 2015. URL: https://weiguanwang.github.io/files/Theses/Master_Dissertation.pdf.